6 Isotopes

Atoms consist of a nucleus and a surrounding cloud of electrons. The nucleus contains positively charged *protons* and anywhere from 0 to over 100 *neutrons* (particles that have nearly the same mass as a proton, but no charge). The number of protons in the nucleus uniquely determines the element—i.e., hydrogen has 1 proton, helium 2 protons, uranium 92 protons, etc. ***Isotopes*** are *atoms that have the same number of protons but a different number of neutrons.* The ***atomic number*** of an element is the *number of protons in the nucleus,* and the ***atomic mass number*** is the *number of protons plus the number of neutrons in the nucleus.* For example, there are three isotopes of hydrogen, ${}_{1}^{1}\mathrm{H}$, ${}_{1}^{2}\mathrm{H}$, and ${}_{1}^{3}\mathrm{H}$, all of which have 1 proton in the nucleus. ${}_{1}^{1}\mathrm{H}$ contains 1 proton and no neutrons, ${}_{1}^{2}\mathrm{H}$ contains 1 proton and 1 neutron, and ${}_{1}^{3}\mathrm{H}$ contains 1 proton and 2 neutrons. By international convention, the number at the bottom left of the element symbol is the atomic number and the number at the upper left of the element symbol is the atomic mass. Often, the atomic number is not attached to the symbol because it is implied by the element name.

It is convenient to divide the isotopes into two groups: radioactive and stable. ***Radioactive isotopes*** are *atoms that undergo spontaneous breakdown of their nuclei to form other isotopes.* ***Stable isotopes*** *do not spontaneously break down to form other isotopes.* Both types of isotopes have a wide range of applications in the physical and biological sciences. In this chapter we will focus on those isotopes that have been found to be particularly useful in describing and characterizing the surface and near-surface environment.

RADIOACTIVE ISOTOPES

Basic Principles

Radioactivity is defined as *the spontaneous breakdown of a nucleus.* This breakdown can follow several pathways: alpha (α) or beta (β^-) particle emission, positron (β^+) particle emission, and K-electron capture (ε). As an example of the different types of decay processes, consider the radioactive decay of ${}_{92}^{238}\mathrm{U}$ (Table 6−1). This uranium isotope contains 92 protons and 146 neutrons. The isotope decays through a series of alpha and beta emissions, ultimately arriving at a stable form of lead $({}_{82}^{206}\mathrm{Pb})$. The first step in the decay chain is the emission of an alpha particle. An ***alpha particle*** *consists of 2 protons and 2 neutrons* (equivalent to a helium nucleus). The

resulting nucleus (a thorium atom) has 90 protons and an atomic mass of 234 ($^{234}_{90}\text{Th}$). This nucleus is radioactive (unstable). The next step in the decay chain is the emission of a ***beta particle*** ***(an electron).*** The beta particle is produced by the breakdown of a neutron to yield a proton and an electron. The result is that the atomic number of the nucleus increases by 1, but there is no change in the atomic mass number. The resulting nucleus is a protactinium atom ($^{234}_{91}\text{Pa}$). This decay process continues until a stable nuclear configuration (in this case, $^{206}_{82}\text{Pb}$) is achieved. As an example of K-electron capture, consider the decay of $^{81}_{36}\text{Kr}$. This isotope decays by capturing an electron from the K-shell. The resulting nucleus ($^{81}_{35}\text{Br}$) has the same atomic mass number, but the atomic number has decreased by 1 due to the conversion of a proton to a neutron. ***Gamma rays*** ***(high-energy electromagnetic radiation)*** are also emitted during the decay process. Following the emission of an alpha or beta particle, the nucleus may be left in an excited state. The return of the nucleus to the ground state is accomplished by the emission of the excess energy as gamma rays. Similar to the case with electronic transitions in the atom yielding characteristic X rays, the gamma rays are characteristic of the nucleus and are the basis of a branch of analytical nuclear chemistry known as gamma ray spectroscopy. Both uranium and thorium are important elements in environmental problems, and various parts of their decay chains have been used in a variety of analytical methods. The complete decay chains for uranium are listed in Table 6–1, and the decay chain for thorium is listed in Table 6–2.

Table 6–1 Uranium Decay Series*

Uranium 238			Uranium 235		
Isotope	Emitted particle	Half-life	Isotope	Emitted particle	Half-life
$^{238}_{92}\text{U}$	α	4.47×10^9 y	$^{235}_{92}\text{U}$	α	7.038×10^8 y
$^{230}_{90}\text{Th}$	β^-	24.1 d	$^{231}_{90}\text{Th}$	β^-	1.063 d
$^{234}_{91}\text{Pa}$	β^-	1.17 min	$^{231}_{91}\text{Pa}$	α	3.248×10^4 y
$^{234}_{92}\text{U}$	α	2.48×10^5 y	$^{227}_{89}\text{Ac}$	β^-	21.77 y

Uranium 238			Uranium 235		
$^{230}_{90}\mathrm{Th}$	α	7.52×10^{4} y	$^{227}_{90}\mathrm{Th}$	α	18.72 d
$^{226}_{88}\mathrm{Ra}$	α	1.60×10^{3} y	$^{223}_{88}\mathrm{Ra}$	α	11.435 d
$^{222}_{86}\mathrm{Rn}$	α	3.8235 d	$^{219}_{86}\mathrm{Rn}$	α	3.96 s
$^{218}_{84}\mathrm{Po}$	α	3.10 min	$^{215}_{84}\mathrm{Po}$	α	1.78×10^{-3} s
$^{214}_{82}\mathrm{Pb}$	β^-	27 min	$^{211}_{82}\mathrm{Pb}$	β^-	36.1 min
$^{214}_{83}\mathrm{Bi}$	β^-	19.9 min	$^{211}_{83}\mathrm{Bi}$	α	2.14 min
$^{214}_{84}\mathrm{Po}$	α	1.64×10^{-4} s	$^{207}_{81}\mathrm{Tl}$	β^-	4.77 min
$^{210}_{82}\mathrm{Pb}$	β^-	22.3 y	$^{207}_{82}\mathrm{Pb}$		Stable
$^{210}_{83}\mathrm{Bi}$	β^-	5.01 d			
$^{210}_{84}\mathrm{Po}$	α	138.38 d			
$^{206}_{82}\mathrm{Pb}$		Stable			

*Data source: Chart of the Nuclides (1989).

Note that in the thorium decay chain (Table 6–2), $^{212}_{83}\mathrm{Bi}$ has two decay paths (branching decay), one by α decay to $^{208}_{81}\mathrm{Tl}$ and the other by β^- decay to $^{212}_{84}\mathrm{Po}$. The bismuth isotopes in the uranium decay chains (Table 6−1) show similar branching decays, but in these chains the alternative path comprises only 0.04% (U-238 chain) and 0.3% (U-235 chain). Thus, the resulting radiogenic progeny are not shown in Table 6–1.

Table 6–2 Thorium Decay Series*

Isotope	Emitted particle	Half-life	Isotope	Emitted particle	Half-life
$^{232}_{90}$Th	α	1.40×10^{10} y	$^{216}_{84}$Po	α	0.145 s
$^{228}_{88}$Ra	β^-	5.76 y	$^{212}_{82}$Pb	β^-	10.64 h
$^{228}_{89}$Ac	β^-	6.15h	$^{212}_{83}$Bi	α (33.7%) β^- (66.3%)	1.009 h
$^{228}_{90}$Th	α	1.913 y	$^{208}_{81}$Tl	β^-	3.053 min
$^{224}_{88}$Ra	α	3.66 d	$^{212}_{84}$Po	α	2.98×10^{-7} s
$^{220}_{86}$Rn	α	55.6 s	$^{208}_{82}$Pb		Stable

*Data source: Chart of the Nuclides (1989).

Radioactive Decay and Growth The decay of a radioactive isotope is a first-order reaction and can be written

$$\frac{dN}{dt} = -\lambda N \qquad (6\text{–}1)$$

where N is the number of unchanged atoms at time t and λ is the radioactive decay constant (instantaneous fraction of atoms decaying per unit time). The negative sign indicates that the number of atoms is decreasing with time. Rearranging this equation,

$$\frac{dN}{N} = -\lambda\, dt \qquad (6\text{–}2)$$

and integrating from $t = 0$ to t and from N_0 to N (N_0 is the number of atoms present at $t = 0$), we get

$$\ln \frac{N}{N_0} = -\lambda t \qquad (6\text{–}3)$$

Taking the antilogs and rearranging gives

$$N = N_0 e^{-\lambda t} \qquad (6\text{–}4)$$

the basic form of the radioactive decay equation.

The ***half-life*** of a radioactive isotope is the *length of time it takes for half of the atoms to spontaneously decay.* Note that this is an exponential relationship. For example, if we start with 1000 atoms, after one half-life 500 will be left, after the second half-life 250 will remain, after the third half-life 125 will remain, etc. The relationship between the decay constant and the half-life can be determined from equation (6–4). After one half-life, $N = N_0/2 = 0.5$ when $N = 1$. Substituting into equation 6–4 gives

$$\frac{1}{2} = \mathrm{le}^{-\lambda t 1/2} \qquad (6\text{–}5)$$

Taking the antilog and rearranging gives

$$t_{1/2} = \frac{\ln 2}{\lambda} = \frac{0.693}{\lambda} \qquad (6\text{–}6)$$

The radioactive decay equation can also be written in terms of activity, i.e., the number of alpha particles or beta particles or gamma rays emitted per unit time.

$$A = A_0 e^{-\lambda t} \qquad (6\text{–}7)$$

where A is the activity at some time t, A_0 is the activity at time zero, and λ is the decay constant. Rearranging this equation, taking the log and solving for t, we get

$$t = \frac{1}{\lambda} \ln \frac{A_0}{A} \qquad (6\text{–}8)$$

Thus, the ratio of the initial activity to the observed activity enables us to determine the radiometric age of the system.

Consider the radioactive decay of $^{238}_{92}\mathrm{U}$ to $^{234}_{90}\mathrm{Th}$. $^{238}_{92}\mathrm{U}$ is the *radioactive parent* and $^{234}_{90}\mathrm{Th}$ is the *radiogenic progeny.* For any closed system at time t, the number of progeny atoms produced plus the number of parent atoms remaining must equal the total number of parent atoms at the start. Returning to equation 6–4 and substituting P for the number of progeny atoms produced, we get another form of the radiometric age equation that is used when both parent and progeny are

measured. Note that N and P are numbers of atoms.

$$N = (N + P)e^{-\lambda t} \qquad (6–9)$$

Rearranging and solving for t gives

$$t = \frac{1}{\lambda} \ln\left[1 + \frac{P}{N}\right] \qquad (6–10)$$

Returning to equation 6–4, we can also describe radioactive decay in terms of the growth of the radiogenic progeny. At any time t the number of radiogenic progeny atoms produced by the decay of the parent is

$$P = N_0 - N \qquad (6–11)$$

Substituting for N, using equation 6–4, gives

$$P = N_0 - N_0 e^{-\lambda t} = N_0(1 - e^{-\lambda t}) \qquad (6–12)$$

The relationship between the growth of the radiogenic progeny and the decay of the radiogenic parent is shown graphically in Figure 6–1. In this example it is assumed that the radiogenic progeny is not itself radioactive.

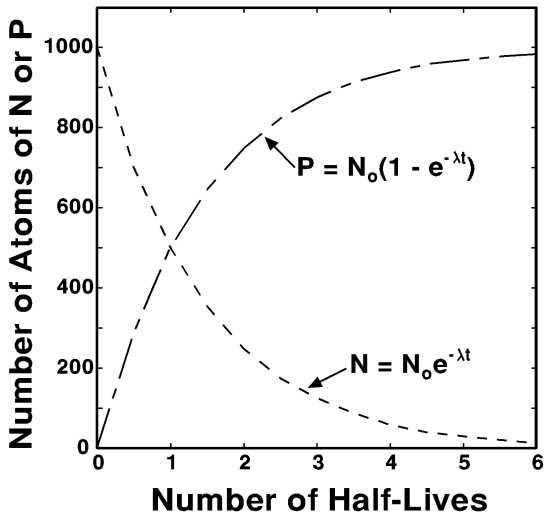

Figure 6–1 Graphical representation of decay of radioactive parent (*N*) and growth of radiogenic progeny (*P*).

If the radiogenic progeny is radioactive (as is the case for all but the last of the radiogenic progeny in the U and Th decay series, Tables 6–1 and 6–2), we need to use a form of the radioactive decay equation that not only considers the growth of the radiogenic progeny but also its decay to another radiogenic progeny. We can rewrite the radioactive decay equation 6–1 in terms of the radiogenic progeny.

$$\frac{dN_2}{dt} = \lambda_1 N_1 - \lambda_2 N_2 \qquad (6\text{–}13)$$

where N_1 is the number of parent atoms, N_2 is the number of radiogenic progeny atoms, and λ_1 and λ_2 are the respective decay constants. Substituting for N_1 and N_2 using equation 6–4, integrating, and taking the antilogs gives

$$N_2 = \frac{\lambda_1}{\lambda_2 - \lambda_1} N_1^0 (e^{-\lambda_1 t} - e^{-\lambda_2 t}) + N_2^0 e^{-\lambda_2 t} \qquad (6\text{–}14)$$

where N_1^0 and N_2^0 are, respectively, the number of radioactive parent and radiogenic progeny atoms present at $t = 0$. If there are no radiogenic progeny atoms initially present, the last term of equation 6–14 is zero. If $\lambda_1 > \lambda_2$, the amount of the progeny will first increase, and then after the parent has disappeared, the amount of the progeny will decrease at a rate determined by its half-life. A more interesting case is when $\lambda_1 < \lambda_2$. In this case, a transient equilibrium will be achieved. This occurs because as the decay time increases, the terms involving $e^{-\lambda 2t}$ become negligible. Equation 6–14 is now written

$$N_2 = \frac{\lambda_1}{\lambda_2 - \lambda_1} N_1^0 e^{-\lambda_1 t} \qquad (6\text{–}15)$$

Substituting $N_1^0 = \frac{N_1}{e^{-\lambda_1 t}}$ (by rearranging equation 6–4) gives

$$\frac{N_1}{N_2} = \frac{\lambda_2 - \lambda_1}{\lambda_1} \qquad (6\text{–}16)$$

If the half-life of the parent is much longer than that of the progeny, i.e., $\lambda_1 << \lambda_2$, equation 6–16 becomes

$$\frac{N_1}{N_2} = \frac{\lambda_2}{\lambda_1} \qquad (6\text{–}17)$$

This last case is an example of secular equilibrium in which the ratio of the number of parent to the number of progeny atoms remains constant. In effect, what has happened is that the rate of decay of the progeny is balanced by the rate of formation of the progeny by the decay of the parent.

Table 6–3 RBE Values for Various Types of Radiation*

Radiation	RBE
X and γ rays	1
Beta rays and electrons	1
Thermal neutrons	2
Fast neutrons	10
Protons	10
Alpha particles	20
Heavy ions	20

*From Cember (1983).

Measurement of Radioactivity The ***becquerel (Bq)*** is the basic unit of measurement for radioactivity, *1 Bq = 1.000 disintegrations* s^{-1}. Radioactivity is often expressed in ***curies (Ci),*** *1 Ci* $= 3.700 \times 10^{10}$ *disintegrations per second.* A picocurie is 1×10^{-12} curies. In the quantitative study of the chemical and biological effects of radiation, a measure of the amount of energy absorbed (the dose) is required. The unit used for the dose is the ***gray (Gy),*** and *a dose of 1 Gy deposits 1 joule of energy per kilogram of material.* Another often-used unit is the *rad:* 1 Gy = 100 rad. The biological effects of radiation are due to changes in the chemistry of the cells. These changes are caused by ionization, excitation, dissociation, and atomic displacement due to the passage of the radiation through the cells. The ***sievert (Sy)*** is the *unit of radiation dosage used to measure the biological effects of radiation.* In the past, the ***rem*** *(roentgen equivalent man)* was the commonly used unit: 1 Sy = 100 rem. The dosage in Sieverts is equal to the dosage in grays multiplied by the ***relative biological effectiveness (RBE),*** *a measure of the ability of various types of radiation to*

cause ionization in biological materials. RBE values for different types of radiation are given in Table 6–3.

Radioactive Isotopes Used in Environmental Studies A number of radioactive isotopes (Table 6–4) have been used in environmental studies to determine the age of groundwater, sediments, and ice cores; to measure groundwater flow rates; and as tracers for groundwater movement. Which isotopic system to use is determined by the nature of the problem. Important parameters are the half-life of the radioisotope and the reactivity of the isotope in the system of interest.

Tritium Dating

There are three isotopes of hydrogen: ${}^{1}_{1}\mathrm{H}$, ${}^{2}_{1}\mathrm{H}$ (deuterium), and ${}^{3}_{1}\mathrm{H}$ (tritium), with average terrestrial abundances (in atomic %) of 99.985, 0.015, and $< 10^{-14}$, respectively. The first two isotopes are stable but tritium is radioactive ($t_{½}$ = 12.43 y) and is produced in the upper atmosphere by the bombardment of nitrogen with cosmic-ray-produced neutrons.

$$ {}^{14}_{7}\mathrm{N} + {}^{1}_{0}n \rightarrow {}^{3}_{1}\mathrm{H} + {}^{12}_{6}\mathrm{C} \qquad (6\text{–}18) $$

With the onset of atmospheric testing of fusion bombs in 1952, bomb-produced tritium became the major source of this isotope. Since the signing of the Atmospheric Test Ban Treaty in 1963, there has been a continual decline in tritium due to the cessation of atmospheric testing and radioactive decay. Tritium abundances are measured in several ways: ***tritium unit (TU) =*** *1 tritium atom per* 10^{18} *hydrogen atoms,* dpm L^{-1} = disintegrations

Table 6–4 Radiometric Isotopes Used in Environmental Studies

Radioactive parent	Radiogenic progeny	Type of decay	Half-life (y)	Decay constant (y^{-1})
${}^{3}_{1}\mathrm{H}$	${}^{3}_{2}\mathrm{He}$	β^-	12.43	5.575×10^{-2}
${}^{14}_{6}\mathrm{C}$	${}^{14}_{1}\mathrm{N}$	β^-	5.73×10^{3}	1.209×10^{-4}
${}^{36}_{17}\mathrm{Cl}$	${}^{36}_{18}\mathrm{Ar}$	β^-	3.01×10^{5}	2.302×10^{-6}
${}^{81}_{36}\mathrm{Kr}$	${}^{81}_{35}\mathrm{Br}$	ε	2.10×10^{5}	3.300×10^{-6}

Radioactive parent	Radiogenic progeny	Type of decay	Half-life (y)	Decay constant (y^{-1})
$^{234}_{92}U$	$^{230}_{90}Th$	α	2.48×10^{5}	2.794×10^{-6}
$^{230}_{90}Th$	$^{226}_{88}Ra$	α	7.52×10^{4}	9.217×10^{-6}
$^{226}_{88}Ra$	$^{222}_{84}Rn$	α	1.622×10^{3}	4.272×10^{-4}
$^{210}_{82}Pb$	$^{210}_{83}Bi$	β^-	22.26	3.11×10^{-2}
$^{231}_{91}Pa$	$^{227}_{89}Ac$	α	3.248×10^{4}	2.134×10^{-5}
$^{87}_{37}Rb$	$^{87}_{38}Sr$	β^-	4.88×10^{10}	1.42×10^{-11}
$^{232}_{90}Th$	$^{208}_{82}Pb$	α, β^-	1.401×10^{10}	4.948×10^{-11}
$^{235}_{92}U$	$^{207}_{82}Pb$	α, β^-	7.038×10^{8}	9.849×10^{-10}
$^{238}_{92}U$	$^{206}_{82}Pb$	α, β^-	4.468×10^{9}	1.551×10^{-10}

ε = K-electron capture.

per minute per liter, and pCi L^{-1} = picocuries per liter (of water). The units are related as follows:

$$1 \text{ TU} = 7.1 \text{ dpm L}^{-1} = 3.25 \text{ pCi L}^{-1} \qquad (6\text{–}19)$$

Prior to the atmospheric testing of fusion devices, the tritium content of precipitation was probably between 2 and 8 TU (Thatcher, 1962). A peak concentration of several thousand TU was recorded in northern hemisphere precipitation in 1963 (Weiss et al., 1979).

EXAMPLE 6–1 *Assume that in 1951, before the first atmospheric tests of fusion bombs, the concentration of tritium in rainwater was 8 TU. Calculate the maximum activity (in pCi L^{-1}) for prebomb tritium in a present-day (2003) groundwater reservoir.*

$$3.25 \text{ pCi L}^{-1} \times 8 \text{ TU} = 26 \text{ pCi L}^{-1}$$

Fifty-two years have elapsed since 1951 (2003 − 1951), and the decay constant for tritium is

$5.575 \times 10^{-2}\ y^{-1}$. Using equation 6−7, we can calculate the present-day activity.

$$A = A_0 e^{-\lambda t} = (26\ \text{pCi L}^{-1}) e^{-(0.05575)(52)} = 1.4\ \text{pCi L}^{-1}$$

For any groundwater sample that had a tritium activity of greater than 1.4 pCi L^{-1}, we would conclude that at least some of the water was added to the reservoir since 1951. ■

The major use of tritium has been to determine the age, flow rates, and mixing of groundwaters. If the water moves rapidly through the vadose zone (the zone in which the pores are filled with air), it will have a tritium content reflecting that of the rainwater. Once it becomes part of the groundwater system, the water is isolated from the atmospheric reservoir and the tritium activity decreases according to the radiometric decay law. Waters that were added to the groundwater reservoir between 1952 and 1963 will have distinctly elevated tritium abundances. These waters form an age marker that can be followed through the groundwater system, an example of what is called ***event dating.*** Other nuclides produced during nuclear bomb testing ($^{36}_{17}\text{Cl}$, $^{89}_{38}\text{Sr}$, $^{90}_{38}\text{Sr}$, $^{133}_{55}\text{Cs}$, $^{137}_{55}\text{Cs}$) can be used in a similar manner. The circulation of water masses formed at the surface of lakes or oceans between 1952 and 1963 can also be traced using their inventory of bomb-created isotopes.

Tritium concentration in rainwater shows a strong geographical and seasonal variation. Tritium content in water vapor over the oceans is low because of exchange with oceanic surface water, which has a low tritium concentration. As the air moves across a continent, it acquires tritium both by evapotranspiration and from the stratosphere. There is also a latitudinal and a seasonal effect each spring that is caused by the breakup of the tropopause (the boundary, at about 10 km, between the lowermost layer of the atmosphere, the troposphere, and the overlying stratosphere) between 30° and 60°N latitude. Stratospheric air, which contains a higher abundance of tritium, mixes with tropospheric air, resulting in a seasonal spike in tritium concentrations in midlatitude precipitation. This combination of factors means that there is significant seasonal and latitudinal variation in tritium abundances in rainwater, which makes it difficult to use tritium alone for precise dating and mixing studies. The most common approach is to use any increased tritium (over the preatmospheric testing background) as an indication that some of the water in the system must have been added since 1952. Other issues involve the modeling of water flow through an aquifer (i.e., piston-flow approaches, reservoir models, compartment models, and

advection-dispersion models). A further discussion of these issues can be found in Plummer et al. (1993).

Many of the problems discussed in the previous paragraph can be avoided by using the ***tritium-helium-3 dating method.*** In this method, both ^3H and its radiogenic progeny, ^3He, are measured. In a confined system, one that is unaffected by dispersion, measurement of both these isotopes allows us to calculate the amount of tritium originally present in the water sample of interest. Potential complications are the presence of sources and sinks for ^3He in the system. Schlosser et al. (1989) suggested the following mass balance equation for ^3He in a groundwater system:

$$^3He_{tot} = {}^3He_{trit} + {}^3He_{eq} + {}^3He_{exc} + {}^3He_{nuc} \qquad (6\text{–}20)$$

where $^3He_{tot}$ is the total ^3He, $^3He_{trit}$ is the tritogenic component, $^3He_{eq}$ is the ^3He added when the water moves through the vadose zone and equilibrates with the air, $^3He_{exc}$ is derived from air entering the groundwater during recharge, and $^3He_{nuc}$ is derived from decay processes, other than the breakdown of tritium, occurring within the system. We will be using TU units for both the radioactive parent and the radiogenic progeny, so we can solve for the age using equation 6–10.

$$t = \frac{1}{\lambda}\ln\left[1+\frac{P}{N}\right] = \frac{1}{5.575\times10^{-2}}\ln\left[1+\frac{^3He_{trit}}{^3H}\right] = 17.937\ln\left[1+\frac{^3He_{trit}}{^3H}\right] \qquad (6\text{–}21)$$

The amount of tritogenic ^3He in a water sample is calculated from the measured $^3He/^4He$ ratio and the concentration of ^4He in the water sample. A correction for the nucleogenic component is done using the amount of neon in the sample, which is assumed to have only an atmospheric source. For further details, the student should read the papers by Schlosser et al. (1988, 1989). Both ^3H and $^3He_{trit}$ concentrations are given in TU (or TR, the tritium ratio: 1 TR – $^3H/H_{tot} = 1 \times 10^{-18}$). Remember that ^{3}Hetrit is produced by the decay of ^3H and the TU for this isotope represents the original amount of ^3H that gave rise to the measured amount of $^3He_{trit}$.

EXAMPLE 6–2 *Water samples are taken from two wells, 100 m apart. Both samples are collected 1 m below the water table. For well #1, ^3H = 25 TU and $^3He_{trit}$ = 0.8 TU. For well #2, ^3H = 20.5 TU and $^3He_{trit}$ = 6.2 TU. Calculate the ages of the water samples. Given that groundwater moves from well #1 to well #2, calculate the rate of groundwater flow.*

Using equation 6–21,

$$\text{Well } \#1: t = 17.937 \ln\left[1 + \frac{0.8}{25}\right] = 0.6 \text{ y}$$

$$\text{Well } \#2: t = 17.937 \ln\left[1 + \frac{6.2}{20.5}\right] = 4.7 \text{ y}$$

Rate of flow = 100 m/(4.7 – 0.6) = 100 m/4.1 y = 24 m y^{-1} ■

In Case Study 6–1 the $^3H/^3H$ dating method is used to determine the time and location of a contaminant release to a groundwater system.

CASE STUDY 6–1 Determination of the Source and Time of Contaminant Release to an Unconfined Gravel Aquifer Using $^3H/^3He$ Dating

High concentrations of benzene and ethylene dibromide (EDB) were encountered in exploratory water wells at the FS-12 field site on Cape Cod, Massachusetts (Figure 6–C1-1). This site is adjacent to the Massachusetts Military Reservation. A road runs through the site and an underground pipeline follows this road. The pipeline was used to transport both aviation gasoline and JP-4 jet fuel. Approximately 2000 gallons of fuel leaked from this pipeline during 1972, and this was thought to be the source of the organic contaminants. However, monitoring wells installed along the roadway and a soil gas survey did not detect contamination.

Solomon et al. (1995) used the $^3H/^3He$ dating method to determine the ages of groundwater at the site and from these ages developed a model that allowed them to determine the location and date of the contaminant release. The site lies within a glacial outwash plain, and groundwater flow occurs within an unconfined gravel aquifer. Five multilevel sampling systems (MLS) were installed on the site (Figure 6–C1-1). In each well, water was collected at various depths and an age determined for each sample. For the leading edge of the contaminant plume, the groundwater age was 16 years. The measurements were made in 1993, so the time at which this groundwater was at the water table would be 1977. Because of dispersion, the leading edge of the contaminant plume moves at a different rate than the groundwater. This difference was estimated to correspond to an age difference of two years, giving the time at which the contaminant was at the water table as 1975. The vertical age profiles were used to determine recharge rates, and these results were then used to estimate horizontal groundwater flow rates. Given the flow rates and the age of the

leading edge of the contaminant plume, an upgradient source for the organic contaminant was identified. Site investigations found fuel floating on the water table in the area identified as the source of the contaminant.

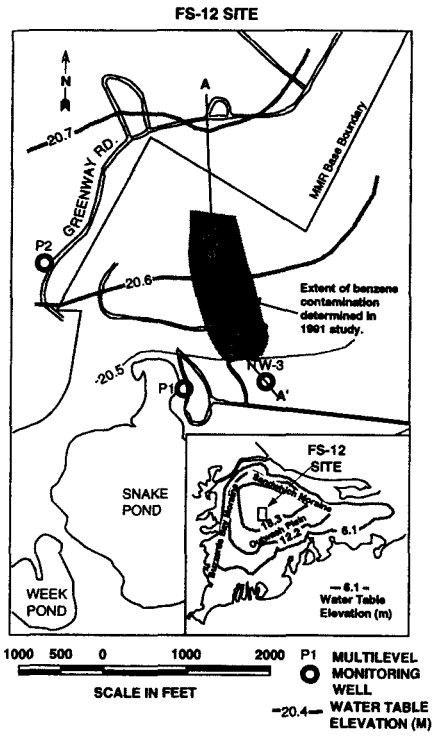

Source: Solomon et al. (1995).

Figure 6–C1-1 *Location and extent of spill. From "Site Characterization using 3H/3He Ground Water Ages, Cape Cod, MA" by D. K. Solomon, R. J. Poreda, P. G. Cook and A. Hunt, GROUND WATER; Vol. 33, No. 6, p. 989 (Figure 1, FS 12). November/December 1995. Reprinted from GROUND WATER with permission of the National Ground Water Association. Copyright 1995.*

Carbon-14 Dating

The tritium dating system can only be used for young (i.e., less than 50-year-old) samples. Thus, there is a need for other isotopic systems that can be used for older samples. One of these is carbon-14, which has been widely used in the geosciences and archaeology. It is the most commonly used system for dating samples less than 50,000 years old. Using accelerator mass spectrometry (AMS), the method can be extended to samples that are greater than 100,000 years old, although care must be taken to ensure that the samples are not contaminated by modern carbon. There are three isotopes of carbon: ${}^{12}_{6}\mathrm{C}$, ${}^{13}_{6}\mathrm{C}$, and ${}^{14}_{6}\mathrm{C}$, with average terrestrial abundances

(in atomic %) of 98.90, 1.10, and < 10^{-10}, respectively. The first two isotopes are stable but $^{14}_{6}\mathrm{C}$ is radioactive ($t_{½}$ = 5730 years) and is produced in the upper atmosphere by the bombardment of nitrogen with cosmic-ray-produced neutrons.

$$^{14}_{7}\mathrm{N} + ^{1}_{0}n \rightarrow ^{1}_{1}\mathrm{H} + ^{14}_{6}\mathrm{C} \qquad (6\text{–}22)$$

The decay of ^{14}C occurs as follows:

$$^{14}_{6}\mathrm{C} \rightarrow {}^{14}_{7}\mathrm{N} + \beta^{-} + \bar{\nu} + Q \qquad (6\text{–}23)$$

where $\boldsymbol{\nu}$ is the antineutrino and Q is the maximum decay energy, 0.156 MeV (million electron-volts) for this reaction. No gamma (y) rays are emitted, so the abundance of the radioactive isotope is determined by beta counting. This is done either by gas counting or liquid scintillation counting. Even for a relatively young sample, the number of beta emissions is small, so great care has to be taken to shield the counter from background radiation. A number of laboratories now do ^{14}C determinations by AMS. In this method, the atoms in the sample are converted to a beam of fast-moving ions. The appropriate mass is then selected through the application of electric and magnetic fields. The advantages of this method are increased sensitivity and much smaller sample size than that required for conventional beta counting methods.

In order to use the ^{14}C system for geochronology, it is assumed that the atmosphere is in ***secular equilibrium*** with respect to ^{14}C. *By this we mean that the rate at which ^{14}C is produced by the cosmic ray flux is balanced by the rate of decay of ^{14}C so that the abundance of ^{14}C in the atmosphere remains constant.* As long as an organism is alive, or water is in contact with the atmosphere, there is a constant exchange of CO_2 between the systems. When the organism dies, or the water becomes isolated from the atmosphere, the ^{14}C content begins to decrease through radioactive decay. The measured activity of a sample at any time t compared to the activity when the system became closed to atmospheric exchange yields the age of the sample. Using equation 6–8, with $\lambda = 1.209 \times 10^{-4}\ \mathrm{y}^{-1}$

$$t = \frac{1}{1.209\times10^{-4}} \ln\left(\frac{A_0}{A}\right) = 8.271\times10^{3} \ln\left(\frac{A_0}{A}\right) \qquad (6\text{–}24)$$

where A_o is the initial activity of the sample at $t = 0$ and A is the activity of the sample at some time t.

EXAMPLE 6–3 *The ^{14}C activity of modern-day carbon is 13.56 dpm g^{-1} of carbon. Charcoal from an ancient campfire has an activity of 6.22 dpm g^{-1} of carbon. Assuming that the wood was only a year or so old when it was burned in this fire, what was the age of the fire?*

$$t = 8.271\times10^3 \ln\left(\frac{A_0}{A}\right) = 8.271\times10^3 \ln\left(\frac{13.56}{6.22}\right) = 6446 \text{ years before present} \quad \blacksquare$$

In practice, the atmospheric concentration of ^{14}C does not remain constant. There are a number of reasons for these variations: (1) addition of significant amounts of ^{14}C to the atmosphere since 1952 due to the testing of nuclear weapons and the operation of reactors and particle accelerators; (2) addition of ^{14}C-depleted carbon through the burning of fossil fuel; (3) changes in the cosmic-ray proton flux; (4) changes in the earth's magnetic field, which modulates proton flux; and (5) climatic changes causing changes in the carbon reservoirs of the earth. A scheme to correct for these ^{14}C variations has been devised using dendrochronology (the study of tree rings). The correction is done by taking long-lived species, such as the bristlecone pine, and determining the ^{14}C content of the various rings. It is assumed that after each ring is formed it is isolated from the atmosphere. Using living trees and preserved logs, it has been possible to extend this correction back about 10,000 years. After making the ^{14}C measurements, ages in this time span are corrected for the atmospheric variations in ^{14}C.

Another problem with ^{14}C dating is isotopic fractionation, a topic that will be more fully developed in a later section of this chapter. Consider the formation of carbonate shell material by a mollusk. CO_2 in the atmosphere is dissolved in seawater and subsequently taken up, along with Ca, by the mollusk to form the shell material. There are a variety of physical, chemical, and biological processes that will cause a change in the relative proportions of the three C isotopes. This is known as *isotope fractionation.* Thus, the shell material will not have the same amount of ^{14}C relative to ^{12}C and ^{13}C as is observed in the atmosphere. In order to minimize this problem, the same species of organism is used for radiocarbon dating. The present-day ^{14}C activity is determined from a living organism, and this activity is compared to that of the ancient shell. This approach is still not without problems because variations in atmospheric ^{14}C must also be taken into account, plus the possibility that there may have been introduction of nonradiogenic carbon into the aquatic system.

There are also several pitfalls in groundwater dating. The starting assumption is that the groundwater was in equilibrium with atmospheric CO_2, yielding an initial ^{14}C activity. This

activity, however, can be changed by various processes within the groundwater system. These include the addition of dissolved organic carbon and inorganic carbon released by the dissolution of limestone. Consider the latter possibility. Suppose the groundwater comes in contact with 100-million-year-old limestone. The limestone contains no ^{14}C. If some of the limestone is dissolved, releasing carbon to the groundwater, the result is a dilution in the concentration of ^{14}C relative to the other carbon isotopes. Consequently, the ^{14}C age of this groundwater would be older than the true age (less ^{14}C per gram of carbon). Conversely, the addition of modem carbon to a sample would increase the amount of ^{14}C relative to the total carbon and hence yield an age younger than the true age.

Despite the possible complications in ^{14}C dating, this is a widely used technique. In many cases, the measured ages must be corrected in various ways, but careful assessment of the variables that can affect the ages often permits an accurate age determination.

U-Series Disequilibrium Methods of Dating

A number of geochronological methods have been developed using various parts of the U (Table 6–1) and Th (Table 6–2) decay chains. We will consider a few of these methods here. More detailed and complete discussions can be found in isotope geochemistry textbooks (Faure, 1986; Dickin, 1997). For a system closed for a sufficiently long time—i.e., secular equilibrium has been achieved—the relative abundance of each isotope in the decay chain will be constant. The basis of the disequilibrium methods of dating is the separation of various isotopes in the decay chain due to differences in their geochemical behavior. This separation can either be a progeny from its parent, with subsequent decay of the progeny, or separation of a parent from its progeny, with subsequent growth of the progeny. The result is that the decay chain is now in disequilibrium and the reestablishment of equilibrium can be used as a dating method.

^{230}Th Dating of Marine Sediments ^{230}Th occurs in the ^{238}U decay chain. Its immediate radioactive parent is ^{234}U. ^{230}Th decays to ^{226}Ra. Due to its oxidation state, U is nonreactive in the marine environment and has a residence time (average length of time an element remains in the ocean) on the order of 500,000 years. Thorium is very reactive in the marine environment and has a residence time of about 300 years. It is removed by adsorption onto the surfaces of solids and by incorporation into authigenic minerals. Given that the addition and removal of U to the ocean is in balance (a steady state has been achieved with respect to this element), ^{230}Th is produced at a

constant rate. ^{230}Th activity is measured as a function of depth in a marine sediment core (the actual measurements are done on leachates so that contributions from silicate minerals are eliminated). As long as there has been no disruption of the sediment layers, the uppermost layer represents the present-day Th deposition to the sediments. Comparison of the Th activity at some depth compared to the surface-layer ^{230}Th activity gives the age of the sediment layer. For ^{230}Th, $t_{½}$ = 75,200 years and $\lambda = 9.217 \times 10^{-6}$ y^{-1}. The ^{230}Th age can be determined using equation 6–8.

$$t = 108,495 \ln\left(\frac{^{230}\text{Th}_{\text{initial}}}{^{230}\text{Th}_{\text{meas}}}\right) \quad (6\text{–}25)$$

EXAMPLE 6–4 *The ^{230}Th activity is measured for a marine sediment core. The top layer of the core has a ^{230}Th activity of 62 dpm. At a depth of 1 m the activity is 28 dpm. Calculate the age of the sediment at a depth of 1 m.*

$$t = 108,495 \ln\left(\frac{^{230}\text{Th}_{\text{initial}}}{^{230}\text{Th}_{\text{meas}}}\right) = 108,495 \ln\left(\frac{62}{28}\right) = 86,246 \text{ y}$$

Assuming a constant sedimentation rate, calculate the rate of sediment accumulation.

$$\text{Rate} = \left(\frac{\text{Sediment thickness}}{\text{Time}}\right) = \left(\frac{1 \text{ m}}{86{,}246 \text{ y}}\right) = \left(\frac{100 \text{ cm}}{86.246 \times 10^3}\right) = 1.16 \text{ cm/1000 y}$$

Note that marine sedimentation rates are usually given in cm/1000 years. ■

^{230}Th/^{232}Th Dating of Marine Sediments ^{232}Th is the radioactive parent for the ^{232}Th–^{208}Pb decay chain. The first step in the chain is the decay of ^{232}Th to ^{228}Ra via an alpha emission with $t_{½}$ = 1.40×10^{10} years. It is assumed that both isotopes of Th are removed simultaneously from seawater and that the ^{230}Th/^{232}Th ratio has been constant for the last several hundred thousand years—both reasonable assumptions. The two isotopes should chemically and physically show the same behavior, so variations in Th removal to the sediments will equally affect both isotopes. Thus, while there may be differences in the absolute concentrations of Th scavenged to the sediments, the initial ^{230}Th/^{232}Th activity ratio will be maintained. Because the half-life of ^{232}Th is orders of magnitude greater than the half-life of ^{230}Th, changes in the activity ratio will be solely due to changes in the abundance of ^{230}Th. Using equation 6–7, we can write

$$\left(\frac{^{230}\text{Th}}{^{232}\text{Th}}\right)=\left(\frac{^{230}\text{Th}}{^{232}\text{Th}}\right)^{0} e^{-\lambda t} \qquad (6\text{–}26)$$

Setting R_0 = (^{230}Th/^{232}Th)^0 and R = (^{230}Th/^{232}Th), the initial and measured activity ratios, and using equation 6–8, we can write

$$t=\frac{1}{\lambda}\ln\left(\frac{R_0}{R}\right)=\frac{1}{9.217\times10^{-6}}\ln\left(\frac{R_0}{R}\right)=108,495\ \ln\left(\frac{R_0}{R}\right) \qquad (6\text{–}27)$$

This system is used exactly the same way as the ^{230}Th system for the dating of sediments except that we are now using activity ratios instead of the activity of ^{230}Th alone.

So far, we have considered what is called *unsupported* ^{230}Th. By this we mean that the isotope has been separated from its radioactive parent (^{234}U) and the change in ^{230}Th activity can be described simply by the decay of this isotope. This is often the case, but there is another possibility that needs to be considered. If some U was also taken up by the sediment, there is a source of new ^{230}Th, and we refer to this as *supported* ^{230}Th (produced by radioactive decay). In this case, we would have a complex relationship in which ^{230}Th would initially decrease and then reach a constant activity when secular equilibrium was achieved. If we can determine the ^{238}U/^{232}Th ratio for the sediment, and if this ratio remained constant throughout the depositional interval, it is possible to correct the measured activities for the addition of supported ^{230}Th. At secular equilibrium, the activity of ^{234}U and ^{238}U would be the same; for each atom of ^{238}U that decays one atom of ^{234}U must decay. If this wasn't the case, then the concentration of ^{234}U or ^{230}Th would change and the system wouldn't be in secular equilibrium. The half-life of ^{238}U is so much longer than that of ^{230}Th that for the purpose of this correction the concentration of ^{238}U can be assumed to remain constant. We rewrite equation 6–26 with a second term on the right that accounts for the addition of ^{230}Th through the decay of ^{238}U.

$$\left(\frac{^{230}\text{Th}}{^{232}\text{Th}}\right)=\left(\frac{^{230}\text{Th}}{^{232}\text{Th}}\right)^{0} e^{-\lambda t}+\left(\frac{^{238}\text{U}}{^{232}\text{Th}}\right)(1-e^{-\lambda t}) \qquad (6\text{–}28)$$

Because the ^{238}U/^{232}Th ratio is essentially constant over a million-year time frame, and the half-life of ^{238}U is orders of magnitude greater than that of ^{230}Th, the growth of ^{230}Th is solely controlled by the decay constant of ^{230}Th. Hence, in equation 6–28, $\lambda = 9.217 \times 10^{-6}$ y^{-1}. As an illustration of the

effect of supported ^{230}Th on age calculations, the ^{230}Th/^{232}Th ratio is calculated (Table 6–5) in 100,000-year increments, assuming that initial ^{230}Th/^{232}Th = 42 and ^{238}U/^{232}Th = 2.

Table 6–5 Calculation of ^{230}Th/^{232}Th for Unsupported and Supported ^{230}Th and Total ^{230}Th

Age 10^5 years	Unsupported	^{230}Th/^{232}Th Ratio Supported	Observed
0	42	0	42
1	16.7	1.20	17.9
2	6.65	1.68	8.33
3	2.64	1.87	4.51
4	1.05	1.95	3.00
5	0.42	1.98	2.40
6	0.17	1.99	2.16
7	0.07	2.00	2.07
8	0.03	2.00	2.03
9	0.01	2.00	2.01
10	0	2.00	2.00

Except for $t = 0$, the observed ^{230}Th/^{232}Th ratio is greater than the unsupported ratio. Hence, an age calculated on the assumption that only unsupported ^{230}Th was present would be younger than the actual age. At about 1 million years, the unsupported ^{230}Th has decayed away while the supported ^{230}Th has achieved secular equilibrium. For sediments older than 1 million years, the ^{230}Th/^{232}Th ratio would be constant.

^{230}Th/^{231}Pa Dating of Marine Sediments This method is very similar to the ^{230}Th/^{232}Th dating technique described in the previous section. ^{231}Pa is produced in the ^{235}U decay chain and has $t_{½} = 3.248 \times 10^4$ y and $\lambda = 2.134 \times 10^{-5}$ y^{-1}. Like thorium, protactinium is rapidly removed from

seawater. If the removal proceeds with equal efficiency, then the activity ratio of ^{230}Th/^{231}Pa varies with time as a function of the difference in the decay constants. For unsupported ^{230}Th and ^{231}Pa,

$$\left(\frac{^{230}\text{Th}}{^{231}\text{Pa}}\right) = \left(\frac{^{230}\text{Th}}{^{231}\text{Pa}}\right)^{0} \frac{e^{-\lambda_{230}t}}{e^{-\lambda_{231}t}} \qquad (6\text{–}29)$$

If the uranium concentration of the leachable fraction of the sediment is negligible, the effective decay constant becomes $\lambda_e = \lambda_{230} - \lambda_{231} = 9.217 \times 10^{-6}\ \text{y}^{-1} - 2.134 \times 10^{-5}\ \text{y}^{-1} = -1.2123 \times 10^{-5}\ \text{y}^{-1}$ and equation (6–29) can be written

$$\left(\frac{^{230}\text{Th}}{^{231}\text{Pa}}\right) = \left(\frac{^{230}\text{Th}}{^{231}\text{Pa}}\right)^{0} e^{\lambda_e t} \qquad (6\text{–}30)$$

where λ_e is now positive and equals $1.2123 \times 10^{-5}\ \text{y}^{-1}$. Because the half-life of ^{230}Th is greater than that of ^{231}Pa, the activity ratio will actually increase as a function of age. If uranium is present in the leachable fraction, then corrections must be applied for supported ^{230}Th and ^{231}Pa, a more complicated problem that will not be discussed here.

Activity and Sedimentation-Rate Relationships Because radioactive decay is a first-order reaction—i.e., the relationship is exponential—even when the sedimentation rate is constant a plot of activity versus sediment depth will yield a curved line (Figure 6–2). However, for constant sedimentation rates a plot of logarithmic activity versus arithmetic sediment depth will yield a straight line (Figure 6–3). In the case of a constant sedimentation rate, the rate can be calculated from the following relationship:

$$a = \frac{\lambda}{-2.303m} \qquad (6\text{–}31)$$

where a is the sedimentation rate, m is the slope of the straight line, and A is the decay constant. If the sedimentation rate is not constant, then a logarithmic activity versus arithmetic depth plot will not yield a straight line (or straight-line segments).

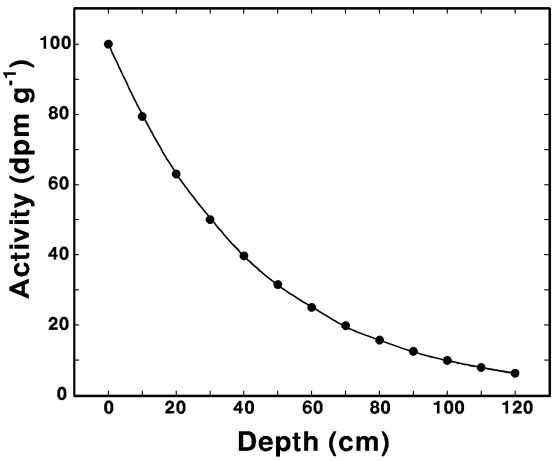

Figure 6–2 Variation of activity with depth at a constant sedimentation rate. Because radioactivity is a first-order reaction, the data define a curved line.

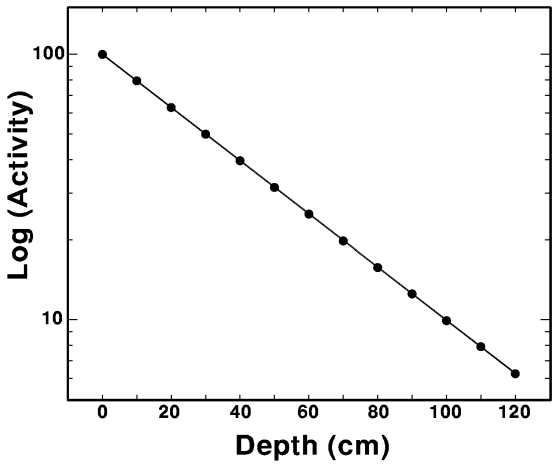

Figure 6–3 Plot of log activity versus depth (arithmetic). For a constant sedimentation rate, the data define a straight line and the sedimentation rate can be determined from the slope of the line (see text). In this case, $m = -0.01003$. If $\lambda = 9.24 \times 10^{-6}$, the sedimentation rate (a) is 4×10^{-4} cm/y = 0.4 cm/1000 y.

---

^{230}Th/^{234}U Dating of Calcium Carbonate This dating system is based on the observation that calcium carbonate formed in the ocean and saline lakes is essentially free of Th but contains significant concentrations (0.1 to 5 ppm) of U. In the ^{238}U decay chain, ^{234}U decays to ^{230}Th via an alpha emission. The half-life for this decay is 2.48×10^5 y with a corresponding decay constant of

2.794×10^{-6} y^{-1}. If the ^{234}U is in secular equilibrium with its parent ^{238}U, the activity of ^{234}U will remain constant with time while the activity of ^{230}Th will increase. Hence, we can use the change in the $^{230}Th/^{234}U$ as a measure of the age of the calcium carbonate. In this case, we are looking at the growth of a radiogenic progeny, rather than its decay, so the decay equation is written

$$\left(\frac{^{230}\text{Th}}{^{234}\text{U}}\right) = 1 - e^{-\lambda t} \qquad (6\text{–}32)$$

which on rearranging and substituting for λ becomes

$$t = \frac{1}{\lambda}\ln\left[1 - \left(\frac{^{230}\text{Th}}{^{234}\text{U}}\right)\right] = 108,495\ \ln\left[1 - \left(\frac{^{230}\text{Th}}{^{234}\text{U}}\right)\right] \qquad (6\text{–}33)$$

In the ocean there is actually a slight excess of ^{234}U; i.e., the $^{234}U/^{238}U$ ratio is 1.15 rather than 1, as would be observed if the two isotopes were in secular equilibrium. If a correction is not made for this excess, the calculated ages are slightly older than the true ages. Once the system has been isolated from seawater, the excess uranium begins to decrease, and after a sufficiently long time the 1:1 ratio expected for secular equilibrium is achieved. Given the 2.48×10^5 y half-life of ^{234}U, it will take more than a million years for secular equilibrium to be reestablished, and the correction to be applied will be a function of the age of the sample.

Why Do We Want to Date Marine Sediments and Carbonate Minerals?

Both ^{14}C and the U-series disequilibrium systems can be used to date marine sediments. Besides our intrinsic interest in earth processes, the dating of marine sediments is essential for climate change studies. At least in the deep ocean, vertical sedimentation is the main depositional process. Typical sediment accumulation rates are on the order of 0.1 to 1 cm/1000 years. Thus, we have a simple stratigraphic record and the potential for a large amount of information to be contained in a relatively short core section of seafloor sediment. Processes at the earth's surface affect the sedimentary record in the deep ocean. For example, variations in the amount of water stored on the continents as ice and surface temperature variations affect a variety of isotopic systems in the ocean (to be discussed later in this chapter). These variations can be used to infer climatic conditions. Additional examples include changes in coarse-fractions deposited in deep-sea sediments due to variations in continental exposure and glacial action and changes in the

distribution of planktonic species in the surface waters (subsequently preserved in the sediment record) in response to changes in the surface temperatures of the ocean. It is generally believed that an understanding of past climates will be important in assessing the potential impact of anthropogenic changes to the earth's present atmosphere. Thus, this is an important area of current research, and it is essential to have good chronological control when interpreting the seafloor sediment record.

^{210}Pb Dating As a final example of U-series disequilibrium dating, we will consider the ^{210}Pb system, which can be used to date a variety of processes occurring during the last 100 years. ^{210}Pb occurs in the ^{238}U–^{206}Pb decay chain. ^{226}Ra decays to ^{222}Rn, which subsequently decays through a series of short-lived daughters to ^{210}Pb. Rn (radon) is a noble gas and rapidly escapes into the atmosphere. Radon decays to ^{210}Pb in a matter of days. The ^{210}Pb is rapidly removed from the atmosphere (mean residence time of about 10 days) by rain or snow. ^{210}Pb is removed from river and ocean water by a combination of inorganic and biochemical reactions. Its mean residence time in the aquatic systems is short, usually less than one year. ^{210}Pb is a short-lived isotope with $t_{½}$ = 22.26 y and $\lambda = 3.11 \times 10^{-2}$ y^{-1}. Assuming that all the ^{210}Pb is unsupported, equation 6–8 can be used to determine the age:

$$t = \frac{1}{3.11\times10^{-2}} \ln\left(\frac{^{210}\text{Pb}^0}{^{210}\text{Pb}}\right) = 32.15 \ \ln\left(\frac{^{210}\text{Pb}^0}{^{210}\text{Pb}}\right) \qquad (6\text{–}34)$$

where ^{210}Pb^0 = the initial activity of ^{210}Pb and ^{210}Pb — the measured (present-day) activity of ^{210}Pb. In principle, this method can be used to determine the age of water samples, the accumulation rate for snow and ice, and sedimentation rates. The presence of U in the sediment can complicate the determination of the sedimentation rate because the decay of ^{238}U will add ^{210}Pb to the sediment (i.e., supported ^{210}Pb). The contribution of supported ^{210}Pb to the total ^{210}Pb activity can be determined by analyzing a sediment sample (a deeper layer in the core) in which all the unsupported ^{210}Pb has decayed or by measuring the activity of ^{226}Ra in each sample and using this activity to calculate the amount of supported ^{210}Pb. Case Study 6–2 describes an application of the ^{210}Pb dating method.

CASE STUDY 6–2 ^{210}Pb Dating of Sediments in Lake Constance, Germany, and Inputs of Pb and Zn to Lake Constance

Bollhöfer et al. (1994) determined the ^{210}Pb ages for two cores from Lake Constance in Germany and used the age distribution to determine the timing of inputs of Pb and Zn to the lake sediments. They also investigated the distribution of radioactive ^{134}Cs, ^{137}Cs, and ^{241}Am in the sediment. The radioactive Cs had two sources: (1) the Chernobyl reactor accident in 1986 and (2) aboveground nuclear weapons testing that produced a Cs maximum in 1963–1964. ^{241}Am is also the result of weapons testing and is produced by the decay of ^{241} Pu to ^{241}Am by emission of a β^- particle. Two sediment cores, which had been previously dated by lamination counting, were used in the study.

The activity of the various radionuclides was determined by gamma ray spectroscopy. The activity due to supported ^{210}Pb was determined by measuring the activity of ^{214}Pb and ^{214}Bi. The source of the supported ^{210}Pb activity is ^{238}U associated with the detrital material in the sediment. ^{214}Pb and ^{214}Bi are both found in the ^{238}U decay chain (Table 6–1), and hence their activity can be used to estimate the supported ^{210}Pb activity. The calculation is done using the equation

$$Act(^{210}\mathrm{Pb}_{\mathrm{excess}}) = Act(^{210}\mathrm{Pb}_{\mathrm{total}}) - Act(^{210}\mathrm{Pb}_{\mathrm{supported}})$$

The ages determined by ^{210}Pb dating, compared to the lamination ages, are shown in Figure 6–C2-1. In general, there is good agreement between the two methods. A logarithmic plot of ^{210}Pb activity versus the compaction-corrected depth gave a mean accumulation rate of 0.16 g cm^{-2} y^{-1}. Two ^{137}Cs maxima were found in the cores, one at a depth of approximately 2 cm, corresponding to the time of the Chernobyl reactor accident, and the other at a depth of approximately 16 cm, corresponding to a ^{210}Pb age of 29 ± 4 y before present (1990$_{present}$ − 29 years = 1961), in agreement, within error, with the time of the Cs maximum from nuclear bomb testing. ^{241}Am also showed a maximum at 16 cm, corresponding to the time of bomb testing. Hence, in this system both bomb-produced radioisotopes proved to be reliable time markers.

The distribution of Pb and Zn in the lake sediments, versus time, is show in Figure 6–C2-2. Preindustrial input of these two metals was determined by measuring the Pb (20 ppm) and Zn (50 ppm) content of the deepest sediment layers, which were deposited before the input of anthropogenic heavy metals. The Pb maximum of approximately 150 ppm and Zn maximum of approximately 330 ppm greatly exceed the preindustrial values. Both maxima are found below the layer with the maximum inventory of bomb-produced radioisotopes. The ^{210}Pb ages of the maxima are 1957 for Pb and 1960 for Zn. Pb released by the burning of leaded gasoline reached a peak (in Germany) in 1971. The Pb maximum in the Lake Constance sediment is 14 years earlier, and at

the time of the Pb atmospheric maximum the Pb in the Lake Constance cores is significantly less than the peak value in 1957. Hence, the Pb (and Zn) input to Lake Constance is from other sources, most likely from the Alpenrhein River, which is the main inlet to Lake Constance, and perhaps from localized atmospheric inputs that reached a maximum in 1957. These sources may be coal burning and the inflow of sewage or sewage sludge through lead pipes.

Source: Bollhöfer et al. (1994).

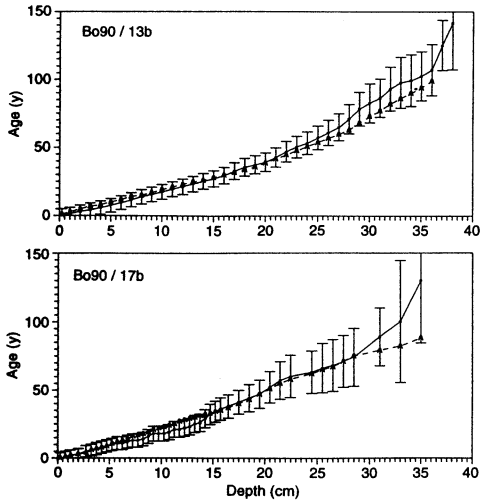

Figure 6–C2-1 *^{210}Pb ages for the two cores using a constant-flux model (solid line) compared to lamination counting (dashed line). From Bollhöfer et al. (1994).*

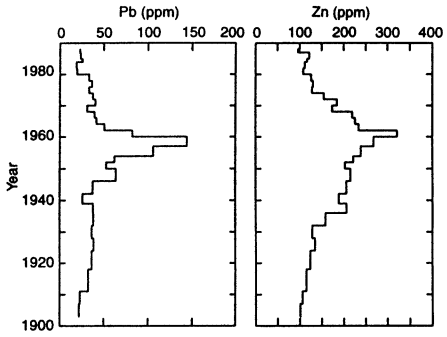

Figure 6–C2-2 *Lead and zinc concentrations versus ^{210}Pb age in sediment core 13b. From Bollhöfer et al. (1994).*

To illustrate the variety of applications of radioisotopes to environmental problems, Case Study 6–3 describes how ^{234}U and ^{238}U isotopes were used to determine the impact of uranium-mill effluent on near-surface groundwater.

CASE STUDY 6–3 Use of ^{234}U and ^{238}U Isotopes to Evaluate Contamination of Near-Surface Groundwater with Uranium-Mill Effluent

Using the $^{234}U/^{238}U$ alpha activity ratio (AR), Zielinski et al. (1997) mapped the extent of uranium contamination in near-surface groundwaters in the vicinity of an abandoned uranium mill. The major aquifers are Quaternary alluvial-terrace deposits and Paleocene sandstones and fluvial conglomerate of the Poison Canyon Formation. Liquid waste (raffinate) and tailings solids stored on the site are the source ot the uranium contamination in the aquifers. Besides high concentrations of uranium, liquid wastes from the site also have high concentrations of molybdenum and selenium. Because of the high concentrations of these elements in some off-site water wells, the site was added to the Superfund National Priority List in 1984.

For the original uranium ore, secular equilibrium was achieved. Thus, the alpha activity of ^{234}U and ^{238}U was the same, giving a theoretical AR = 1. Measured values for liquid waste ranged from 0.98 to 1.05. Most natural groundwater has AR > 1, ranging up to 3 and in some cases up to > 10. The excess ^{234}U is believed to be due to the fact that alpha-recoil displacement occurs when ^{238}U decays to ^{234}U. This displacement damages the crystal structure in the vicinity of the ^{234}U atom and this site is more easily leached during mineral/water interactions. Three background samples from the alluvial aquifer had AR values ranging from 1.32 to 1.41. The groundwaters were found to have a high oxygen content. Thus, the waters are oxidizing and U (and Mo) are expected to remain in solution.

The AR and U concentration for various groundwater samples from the area are shown in Figure 6–C3-1. The field labeled "Range of raffinate activity ratio" shows the range in uranium concentrations and AR expected for raffinate (liquid waste) from the abandoned uranium plant. The field labeled "Range of background activity ratio" shows the range in uranium concentrations and AR expected for uncontaminated groundwater. The field between represents groundwater samples that consist of a mixture of raffinate and uncontaminated groundwater. The dashed lines are mixing lines for various combinations of raffinate and uncontaminated groundwater. The relative volumes of the two end members in the mixed water can be determined from the following relationship:

$$V_1 / V_m = (S_1 / S_m) \times [(AR_2 - AR_m) / (AR_2 - AR_1)]$$

where V_1 is the volume of end member 1, V_m is the volume of the mixed water (this ratio gives the proportion of end member 1 in the mixed water), S = 1/uranium concentration, AR is the alpha activity ratio, and subscripts 1, 2, and m represent end member 1, 2, and the mixed water, respectively. An areal plot of the AR values from the various groundwater samples showed a plume of dissolved uranium that originated in the vicinity of the old tailings ponds and extended northward into the alluvial aquifer. The uranium plume as defined by AR values did not extend as far downgradient as the molybdenum plume (defined by elevated Mo concentrations in the groundwater), suggesting that uranium may be less mobile than molybdenum in the alluvial aquifer.

Source: Zielinski et al. (1997).

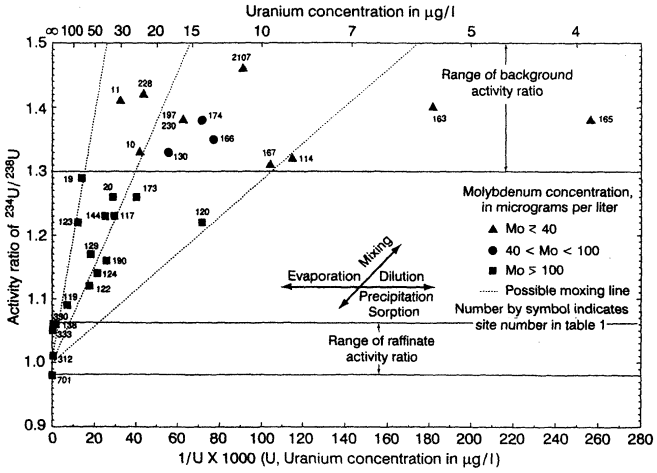

Figure 6–C3-1 *Relationship between AR and U content of groundwater samples and raffinate. The effect of various processes on these values is illustrated in the figure. Evaporation and dilution (or sorption) will change the total uranium concentration. Only mixing will change the AR values. From Zielinski et al. (1997).*

Radiogenic Isotopic Tracers

Radiogenic isotopic tracers are widely used in the geosciences. Several of these isotopic systems have environmental applications. For example, the isotopic composition of Sr in groundwaters can be used to infer the source(s) of the groundwaters. Similarly, the isotopic composition of Pb, a widespread and significant contaminant, can be used to infer the source of the Pb. In this section we will briefly consider the Rb-Sr and U-Th-Pb isotopic systems.

Rb-Sr System There are two naturally occurring isotopes of Rb: $^{87}_{37}\mathrm{Rb}$ (72.654%) and $^{85}_{37}\mathrm{Rb}$ (27.8346%). $^{87}_{37}\mathrm{Rb}$ is radioactive and decays to $^{87}_{39}\mathrm{Sr}$ via a beta emission. There are four naturally occurring isotopes of Sr: $^{88}_{38}\mathrm{Sr}$ (82.53%), $^{87}_{38}\mathrm{Sr}$ (7.04%), $^{86}_{38}\mathrm{Sr}$ (9.87%), and $^{84}_{38}\mathrm{Sr}$ (0.56%). Note that these are only approximate percentages because the amount of $^{87}_{38}\mathrm{Sr}$ produced by radioactive decay will vary from sample to sample. This isotopic system is used in the geosciences to determine the age of igneous and metamorphic rocks, but given the long half-life, it is not a useful system for dating environmental processes. Our interest here is in the variations in the amount of $^{87}_{38}\mathrm{Sr}$ in various reservoirs. Mass spectrometers can very precisely measure mass ratios, so we generally measure the amount of the radioactive parent and radiogenic progeny relative to a stable isotope of the element of interest. Thus, the change in radiogenic Sr with time can be represented by the following equation:

$$\left(\frac{^{87}\mathrm{Sr}}{^{86}\mathrm{Sr}}\right)_{\mathrm{meas}} = \left(\frac{^{87}\mathrm{Sr}}{^{86}\mathrm{Sr}}\right)_{\mathrm{initial}} + \left(\frac{^{87}\mathrm{Rb}}{^{86}\mathrm{Sr}}\right)(e^{\lambda t} - 1) \qquad (6\text{–}35)$$

where $(^{87}\mathrm{Sr}/^{86}\mathrm{Sr})_{\mathrm{meas}}$ is the measured Sr isotopic ratio for the sample, $(^{87}\mathrm{Sr}/^{86}\mathrm{Sr})_{\mathrm{initial}}$ is the Sr isotopic ratio for Sr present in the sample when it was formed, $(^{87}\mathrm{Rb}/^{86}\mathrm{Sr})$ is the present-day isotopic ratio, λ is the decay constant, and t is the time that has elapsed since the sample was formed. Note that the two major factors determining the present-day Sr isotopic ratio for the sample are the $^{87}\mathrm{Rb}/^{86}\mathrm{Sr}$ ratio and the time that has elapsed since the sample was formed.

During the process of crust formation, melts are extracted from the mantle of the earth and added to the crust. Because of differences in the partitioning of Rb and Sr between solid mantle phases (i.e., minerals) and melt, Rb is preferentially enriched with respect to Sr in the melt. The higher Rb/Sr ratio for the melt ultimately leads to higher $^{87}\mathrm{Sr}/^{86}\mathrm{Sr}$ ratios for the crust, which is formed either directly by crystallization of the melt or indirectly by rock weathering. For the same Rb/Sr ratio, the greater the age of the crust, the greater the $^{87}\mathrm{Sr}/^{86}\mathrm{Sr}$ ratio. Conversely, for the mantle from which the melt was extracted (depleted mantle), the growth in $^{87}\mathrm{Sr}$ with time is less than that for the mantle from which a melt has not been extracted (undepleted mantle). The result is a number of Sr isotopic reservoirs with different $^{87}\mathrm{Sr}/^{86}\mathrm{Sr}$ ratios.

As another example of Sr isotopic variability, let us briefly consider what might happen to the

Sr isotopic composition of ocean waters throughout geologic time. The Sr found in the oceans comes from rock weathering and submarine volcanism (see Chapter 10 for a discussion of marine chemistry). As the relative proportions of these contributions vary, and as time progresses, the Sr isotopic composition of the ocean will change. This change is preserved in marine carbonates that formed at different times throughout earth history. Relative to Rb, calcite is highly enriched in Sr (this is because of the crystal structure of calcite, see Chapter 7), and the Sr isotopic ratio of the marine carbonate is approximately the same as the seawater from which it formed. Thus, it has been possible to determine the $^{87}Sr/^{86}Sr$ ratios of ocean waters as a function of time. This has been, and continues to be, an active area of research because the marine Sr isotopic curve can be used for correlation of marine carbonates. Our interest here, however, is the observation that marine carbonates formed at different times in earth history have different Sr isotopic ratios. Thus, there are a number of ways to produce isotopically distinct reservoirs. Sr found in waters in equilibrium with these different reservoirs would have different $^{87}Sr/^{86}Sr$ ratios, thus fingerprinting the source(s) of the waters.

Th-U-Pb Isotopic Systems We have already discussed the U (Table 6–1) and Th (Table 6–2) decay schemes. All three decay schemes end with a lead isotope. Of the naturally occurring Pb isotopes, only ^{204}Pb is nonradiogenic. As we did for Sr, we can write equations that represent the change in radiogenic Pb isotopic composition with time, and in this case we will use ^{204}Pb as the reference lead isotope.

$$\left(\frac{^{206}\text{Pb}}{^{204}\text{Pb}}\right)_{\text{meas}} = \left(\frac{^{206}\text{Pb}}{^{204}\text{Pb}}\right)_{\text{initial}} + \left(\frac{^{238}\text{U}}{^{204}\text{Pb}}\right)(e^{\lambda_{238}t} - 1) \qquad (6\text{–}36)$$

$$\left(\frac{^{207}\text{Pb}}{^{204}\text{Pb}}\right)_{\text{meas}} = \left(\frac{^{207}\text{Pb}}{^{204}\text{Pb}}\right)_{\text{initial}} + \left(\frac{^{235}\text{U}}{^{204}\text{Pb}}\right)(e^{\lambda_{235}t} - 1) \qquad (6\text{–}37)$$

and

$$\left(\frac{^{208}\text{Pb}}{^{204}\text{Pb}}\right)_{\text{meas}} = \left(\frac{^{208}\text{Pb}}{^{204}\text{Pb}}\right)_{\text{initial}} + \left(\frac{^{232}\text{U}}{^{204}\text{Pb}}\right)(e^{\lambda_{232}t} - 1) \qquad (6\text{–}38)$$

where λ_{238} is the decay constant for ^{238}U, λ_{235} is the decay constant for ^{235}U, and λ_{232} is the decay constant for ^{232}Th. As was the case for Sr, the Pb isotopic ratios for a particular sample depend

upon the U/Pb and Th/Pb ratios and the time that has elapsed since the sample was formed. Hence, isotopic reservoirs with different U/Pb and Th/Pb ratios formed at different times will have different Pb isotopic ratios.

Our interest here is anthropogenic lead. Anthropogenic lead is derived from lead ore deposits, and the lead ore mineral is galena (PbS). U and Th do not occur in galena because they are excluded by the crystal structure (see Chapter 7). Thus, the galena freezes-in the Pb isotopic ratios that existed at its time of formation. As was the case for the Sr isotopic system, the Pb isotopic ratios increase with time. Thus, ore deposits formed at different times in earth history have different Pb isotopic ratios. These differences can be used to fingerprint the source of the Pb. This topic is revisited in some detail in Chapters 8 and 10.

STABLE ISOTOPES

Stable isotopes do not spontaneously break down to form other isotopes. They are useful in environmental and geological studies because physical, chemical, and biological processes can lead to changes in the isotopic ratios. These changes arise because of the mass differences between the isotopes. The effects are most noticeable for isotopes that have large relative mass differences. Hence, most of the elements used for stable isotope studies have a low atomic number and atomic mass (Table 6–6). For isotopes with an atomic mass of greater than 40, the relative mass differences are too small for any measurable isotopic fractionation. Most elements used in radiometric dating have high atomic mass, and mass fractionation is not significant. Note, however, that in the previous section we did describe several dating systems that involve low-atomic-number elements. Particularly in the case of ^{14}C dating using carbonate shells, there can be significant fractionation of ^{14}C between the shell material and the water from which the carbon is extracted. To partly compensate for this effect, ^{14}C analyses should only be done on shells from the same species.

Table 6–6 Average Terrestrial Abundances of Stable Isotopes Used in Environmental Studies*

Element	Isotope	Average terrestrial abundance (atom %)
Hydrogen	$^{1}_{1}H$	99.985
	$^{2}_{1}H$	0.015
Carbon	$^{12}_{6}C$	98.9
	$^{13}_{6}C$	1.1
Nitrogen	$^{14}_{7}N$	99.63
	$^{15}_{7}N$	0.37
Oxygen	$^{16}_{8}O$	99.762
	$^{17}_{8}O$	0.038
	$^{18}_{8}O$	0.2
Sulfur	$^{32}_{16}S$	95.02
	$^{33}_{16}S$	0.75
	$^{34}_{16}S$	4.21
	$^{36}_{16}S$	0.014

*Data source: IUPAC (1992).

Basic Principles

Stable Isotope Fractionation Isotopic fractionation is the partitioning of isotopes during physical (evaporation, condensation, melting, crystallization, absorption and desorption, diffusion), chemical, or biological processes. This partitioning is proportional to the difference in the masses

of the isotopes. The processes can either be ***equilibrium reactions,*** in which *forward and backward reaction rates are equal for each isotope,* or ***kinetic reactions,*** which are *unidirectional reactions in which reaction rates are dependent on the masses of the isotopes and their vibrational energies.*

As an example of an equilibrium reaction, consider the evaporation of water into a closed space. At equilibrium, the forward and backward rates of the reaction will be the same, but the isotopic ratios in each phase (liquid and vapor) will be different. There are six possible isotopic combinations for H_2O molecules: $^1H_2{}^{16}O$, $^1H^2H^{16}O$, $^2H_2{}^{16}O$, $^1H_2{}^{18}O$, $^1H^2H^{18}O$, and $^2H_2{}^{18}O$, with atomic masses, respectively, of 18, 19, 20, 20, 21, and 22. We have ignored ^{17}O because of its low abundance. Water molecules move from the liquid to vapor phase when their energy is sufficiently high to overcome the electrostatic attractions that tend to hold the molecules together in the liquid phase. From basic physics: kinetic energy = ½mass × velocity^2. For any given amount of energy, the isotopically lighter molecule will have a greater velocity than the isotopically heavier molecule. Thus, we would expect the isotopically lighter molecule to preferentially escape to the vapor phase. The result is that the vapor phase becomes enriched in the lighter isotopes (^1H and ^{16}O) relative to the liquid.

As an example of a kinetic reaction, consider the breakdown of limestone ($CaCO_3$), on the addition of acid, to Ca^{2+} and CO_2 gas. This reaction is unidirectional—the CO_2 gas escapes and thus does not equilibrate with the solid phase. During a chemical reaction the lighter isotope is more reactive and is concentrated in the reaction products. The relative loss of the lighter isotope from the reactants leads to an enrichment of the reactants in the heavier isotope. The lighter isotope is more reactive because it has a higher vibrational en-ergy and thus a weaker bond. In this example, the gas phase (product) is enriched in the lighter isotopes of C and O, and the enrichment is significantly greater than that which would occur during an equilibrium reaction.

Fractionation Factor The partitioning of stable isotopes between two substances, A and B, is described by the ***isotopic fractionation factor, α.*** The fractionation factor is written

$$\alpha = \frac{R_A}{R_B} \qquad (6\text{–}39)$$

where R_A is the ratio of the heavy to the light isotope in molecule or phase A and R_B is the ratio of

the heavy to the light isotope in molecule or phase B. The fractionation factor varies as a function of temperature. As an example, consider the evaporation of water (Figure 6–4). ^{16}O is enriched in the vapor phase relative to the liquid. Conversely, ^{18}O is enriched in the liquid relative to the vapor, and thus the fractionation factor is greater than 1. With increasing temperature, the fractionation factor decreases, and it becomes 1 at infinite temperature. This happens because at high temperatures the isotopic species are well mixed. Isotopic fractionation factors can be determined either experimentally or calculated from spectroscopic data. In practice, most isotopic fractionation factors are determined empirically from a large set of observational data or by comparisons of natural materials to experimental results obtained in the laboratory.

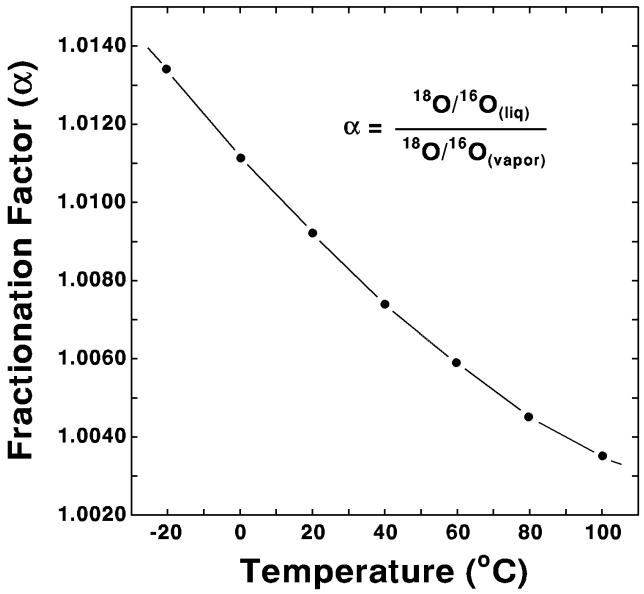

Figure 6–4 Variation of the isotope fractionation factor for oxygen, as a function of temperature, during the evaporation of water. Note that with increasing temperature the fractionation factor approaches 1.0000. Values from Dansgaard (1964).

The isotopic fractionation factor is related to the equilibrium constant of a reaction as follows:

$$\alpha = K^{1/n} \qquad (6\text{–}40)$$

where K is the equilibrium constant and n is the number of atoms exchanged. Consider the carbonate exchange reaction between solid calcium carbonate and water. This particular reaction is of interest because it is used as a paleothermometer in the marine system. Writing the reaction in

terms of a single oxygen, so $n = 1$ in equation 6–40,

$$\frac{1}{3}\mathrm{CaC^{16}O_3} + \mathrm{H_2{}^{18}O} \rightleftharpoons \frac{1}{3}\mathrm{CaC^{18}O_3} + \mathrm{H_2{}^{16}O} \qquad (6\text{–}41)$$

Writing this equation in terms of the equilibrium constant, *K*,

$$K = \frac{[\mathrm{CaC^{18}O_3}]^{1/3}[\mathrm{H_2{}^{16}O}]}{[\mathrm{CaC^{16}O_3}]^{1/3}[\mathrm{H_2{}^{18}O}]} = \frac{([\mathrm{CaC^{18}O_3}]/[\mathrm{CaC^{16}O_3}])^{1/3}}{[\mathrm{H_2{}^{18}O}]/[\mathrm{H_2{}^{16}O}]} \qquad (6\text{–}42)$$

and

$$K = \alpha = \frac{\mathrm{R_c}}{\mathrm{R_w}} = \frac{{}^{18}\mathrm{O}/{}^{16}\mathrm{O} \text{ ratio of calcium carbonate}}{{}^{18}\mathrm{O}/{}^{16}\mathrm{O} \text{ ratio of water}} \qquad (6\text{–}43)$$

Because the isotopic fractionation factor varies as a function of temperature, the measured fractionation factor can be compared to the experimental values to determine the equilibrium temperature for the calcium carbonate-water reaction. In practice, this calculation is a bit more complicated, as will be discussed in a later section.

The δ (Delta) Notation Because isotopic variations are very small, isotopic ratios are written using the delta notation.

$$\delta = \left(\frac{\text{Isotopic ratio of sample} - \text{Isotopic ratio of standard}}{\text{Isotopic ratio of standard}} \right) \times 1000 \qquad (6\text{–}44)$$

A variety of standards are used for comparison (see Table 6–7): ***SMOW*** (standard mean ocean water), ***V-SMOW*** (Vienna standard mean ocean water), and ***SLAP*** (standard light Antarctic precipitation) for oxygen and hydrogen isotope ratios in water; ***PDB*** (PeeDee beleminite) for oxygen and carbon isotope ratios in carbonates; ***AIR*** (air) for nitrogen; and ***CDT*** (Canyon Diablo troilite) for sulfur. PDB is now exhausted so a new standard, ***NBS-19*** (National Bureau of Standards, now NIST), has been established for carbon and oxygen in carbonates. The new standards are related to PDB as follows: $\delta^{18}O_{\text{NBS-19/V-PDB}} = -2.20$ and $\delta^{13}C_{\text{NBS-19/V-PDB}} = 1.95$ (O'Neil, 1986). If the sample is enriched in the heavier isotope relative to the standard, the delta values are positive. If the sample is depleted in the heavier isotope relative to the standard, the delta values are negative.

Table 6–7 Stable Isotope Ratios for Standards*

Element	Standard	Ratio
Hydrogen	V-SMOW	$^{2}H/^{1}H = 155.76 \times 10^{-6}$
Carbon	PDB	$^{13}C/^{12}C = 1123.75 \times 10^{-5}$
Oxygen	V-SMOW	$^{18}O/^{16}O = 2005.2 \times 10^{-6}$
	PDB	$^{18}O/^{16}O = 2067.2 \times 10^{-6}$
Nitrogen	NBS-14	$^{15}N/^{14}N = 367.6 \times 10^{-5}$
Sulfur	CDT	$^{34}S/^{32}S = 449.94 \times 10^{-4}$

*Data from Kyser (1987).

EXAMPLE 6–5 *The isotopic ratio of $^{18}O/^{16}O$ in V-SMOW is 0.0020052. A rainwater sample collected in Boston, Massachusetts, has an $^{18}O/^{16}O$ ratio of 0.0019750. Calculate the delta value for this rainwater sample.*

$$\begin{aligned}\delta &= \left(\frac{\text{Ratio}_{\text{sample}} - \text{Ratio}_{\text{standard}}}{\text{Ratio}_{\text{standard}}}\right)\times 1000 = \left(\frac{0.0019750 - 0.0020052}{0.0020052}\right)\times 1000 \\ &= -15.1‰\end{aligned}$$

The delta value is reported in parts-per-thousand (‰), and the negative value means that the sample is isotopically lighter than the standard. ■

In practice, isotopic ratios are usually measured with respect to the appropriate standard and the results are reported directly in delta values. Because isotopic measurements are reported in delta values, it is useful to derive a relationship that relates the measured delta values to the isotopic fractionation factor. From equation 6–44,

$$R_a = \frac{\delta_a R_{std}}{10^3} + R_{std} = \frac{R_{std}(\delta_a + 10^3)}{10^3} \qquad (6–45)$$

Substituting for R_A and R_B in equation 6–39 gives

$$\alpha_b^a = \frac{R_a}{R_b} = \frac{10^3 R_{std}\left(\delta_a + 10^3\right)}{10^3 R_{std}\left(\delta_b + 10^3\right)} = \frac{\delta_a + 1000}{\delta_b + 1000} \qquad (6\text{–}46)$$

EXAMPLE 6–6 *The oxygen isotopic fractionation factor for the evaporation of water under equilibrium conditions at 25°C is 1.0092 (Craig and Gordon, 1965). Calculate the δ-value for vapor in equilibrium with lake water having a δ-value = −5.0‰. From equation 6−46,*

$$\alpha_v^1 = 1.0092 = \frac{R_1}{R_v} = \frac{\delta_1 + 1000}{\delta_v + 1000}$$

Rearranging and solving for δ_v*,*

$$\delta_v = \frac{\delta_1 + 1000}{\alpha_v^1} - 1000 = \frac{-5 + 1000}{1.0092} - 1000 = -14.1‰ \quad \blacksquare$$

Oxygen and Hydrogen Isotopes in Water

Water molecules consist solely of hydrogen and oxygen so both isotopes usually show similar fractionation patterns, and hence we will consider both elements in the following discussion. Because these elements *are* water, they make ideal tracers for water. Different waters have different isotopic signatures, and these can be used to trace the source(s) of a water mass and/or to provide information on processes within the hydrologic cycle. The source of water and its movement through surface and ground water systems is essential information for studies involving water contamination. A number of factors are responsible for the variations in water isotopic chemistry and these are considered next.

Factors Affecting the Isotopic Composition of Water As described in a previous section and illustrated in Figure 6–4, isotopic fractionation factors vary as a function of temperature. For seawater at 25°C, the isotopic fractionation factors for oxygen and hydrogen are α_{18} = 1.0092 and $\alpha_{\mathbf{D}}$ = 1.074 (Craig and Gordon, 1965). The ^{2}H isotope of hydrogen is called deuterium, and the isotopic ratio is often written D/H, where H stands for common hydrogen (^{1}H) and D stands for deuterium. The isotopic fractionation factor for hydrogen is often written with a D subscript. Given that seawater has a delta value of zero for both isotopes, solving equation 6–46 for the vapor phase yields δ_{18} = −9.1‰ and δ_D = −69‰ for vapor in equilibrium with seawater. At 10°C, δ_{18} = −10.1‰ and δ_D = −84‰, illustrating the effect temperature has on isotopic fractionation. Also note

that both the absolute delta values and the change in delta values are much greater for hydrogen. This is because the relative mass differences are much greater for hydrogen than oxygen. Thus, one factor that will affect isotopic ratios for water vapor and precipitation is temperature variation. This temperature variation can be either latitudinal (higher latitudes equal lower temperatures) or altitudinal (higher altitudes equal lower temperatures). Note that these calculations assume an equilibrium reaction. Actual values for water vapor over the ocean are on the order of −13‰ to −14‰, indicating that the evaporative process is a kinetic reaction rather than an equilibrium reaction (see later).

When raindrops form in a cloud they are enriched in ^{18}O and D relative to the coexisting vapor phase. The first droplets will have an isotopic composition similar to that of ocean water, the exact value depending on the temperature at which the condensation process occurs. Conversely, during condensation the water vapor will become enriched in ^{16}O and ^{1}H. As condensation continues, the water vapor will become progressively isotopically more negative and there will be a corresponding change in the isotopic composition of the water droplets. This process can be described by the Rayleigh distillation equation (Broecker and Oversby, 1971)

$$\frac{R}{R_0} = f^{(\alpha-1)} = \frac{\delta^{18}O + 1000}{\delta^{18}O_0 + 1000} \quad (6\text{–}47)$$

where R is the $^{18}O/^{16}O$ ratio of the water vapor at any point during the condensation process, R_O is the $^{18}O/^{16}O$ ratio of the vapor before condensation begins, f is the fraction of water vapor remaining, and α is the fractionation factor R_l/R_v. We can rewrite equation 6−47 in terms of the $\delta^{18}O$ value of the water vapor:

$$\delta^{18}O_v = [\delta^{18}O_0 + 1000] f^{(\alpha-1)} - 1000 \quad (6\text{–}48)$$

To calculate the $\delta^{18}O$ value for the condensate in equilibrium with the vapor at any instant,

we solve equation 6–46 for the $\delta^{18}O$ value of the liquid by setting R_a = the liquid ratio and R_b = the vapor ratio:

$$\delta^{18}O_l = \alpha(\delta^{18}O_v + 1000) - 1000 \quad (6\text{–}49)$$

The changes in isotopic compositions for both vapor and liquid, assuming a Rayleigh distillation model, are illustrated in Figure 6–5. The initial water vapor has $\delta^{18}O$ = −13‰ and the reaction

takes place at 25°C (α = 1.0092).

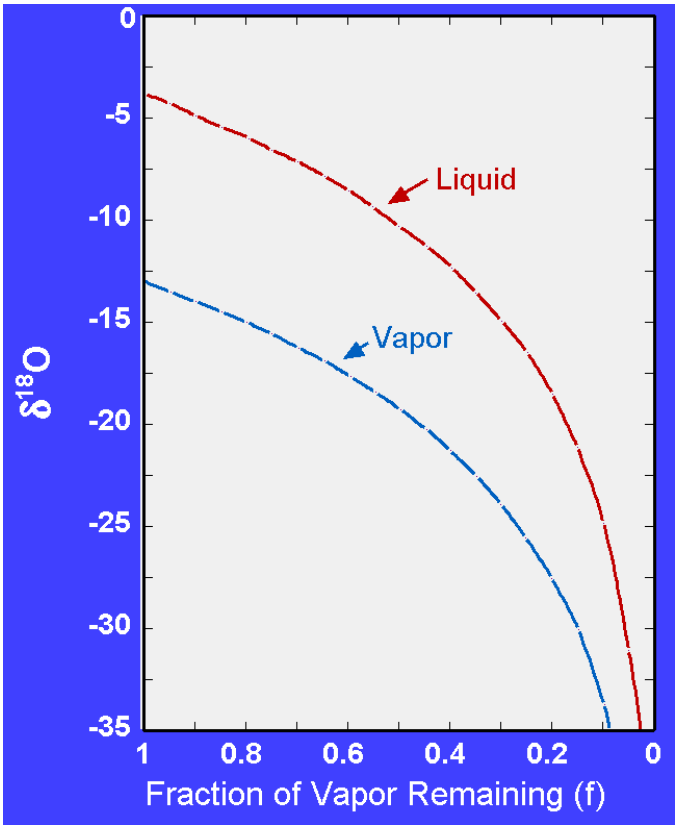

Figure 6–5 Fractionation of oxygen isotopes during Rayleigh distillation of water vapor at 25°C. The initial $\delta^{18}O$ value of the vapor is – 13‰.

As condensation proceeds, both the vapor and the liquid become isotopically lighter. Thus, the isotopic composition of rainwater changes during a precipitation event; i.e., earlier precipitation is isotopically heavier than later precipitation. One outcome of this process is that the delta values of rain tend to decrease as one moves inland from a continental margin. With subsequent reevaporation and reprecipitation, there is a continuing decrease in the delta values for rainwater. Thus, as one moves poleward the rain becomes isotopically lighter, a latitudinal effect that is also enhanced by the decline in ambient atmospheric and seawater temperatures. On the basis of a large number of analyses of meteoric waters collected at different latitudes, Craig (1961) was able to show there was a relationship between the $\delta^{18}O$ and δD values that could be represented by the equation

$$\delta D = 8\delta^{18}O + 10 \qquad (6–50)$$

This relationship defines the mean global meteoric water line (Figure 6–6). Also note that in equation 6–50 there is an excess in δD**.** Dansgaard (1964) found that there was a good correlation between the $\delta^{18}O$ values of average annual precipitation and the average annual air temperature. More generally, we can write equation 6–50 as

$$\delta D = 8\delta^{18}O + d \qquad (6–51)$$

where d = the deuterium excess.

Equation 6–50 defines isotopic variations on a global basis; on a local basis each area has its own meteoric water line (Figure 6–6). These plots are usually made by setting the slope of the straight line to 8, although regression of the actual data may yield slopes other than 8. In these plots excess deuterium varies from 0‰ to +22‰ and cool and humid areas have the lower values. Thus, it may be possible to use differences in the *d*-value to tag water masses. For example, during Pleistocene glaciation meteoric waters had a lower deuterium excess (Merlivat and Jouzel, 1979), which might be used to identify waters recharged to an aquifer during the Pleistocene.

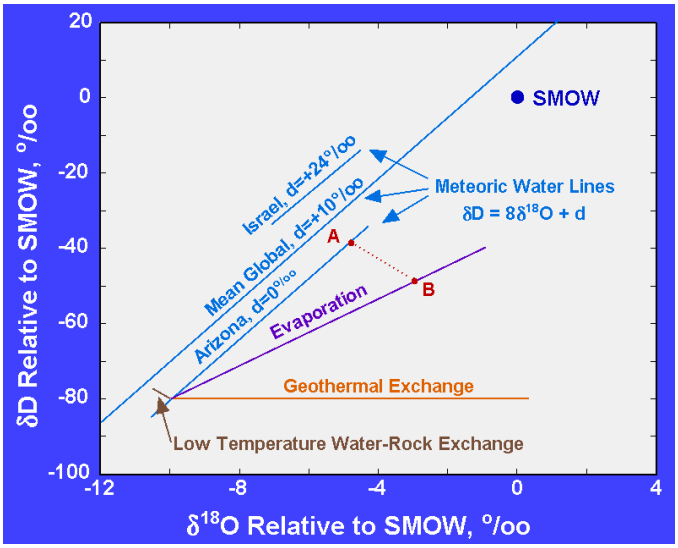

Figure 6–6 Plot of δD versus $\delta^{18}O$ illustrating the mean global meteoric water line and local meteoric water lines. Other processes that affect the isotopic ratios—e.g., low-temperature water-rock exchange, geothermal exchange, and evaporation—are also illustrated. A and B are two water masses and the dashed line represents the possible isotopic compositions of water produced by the simple mixing of these two end members. The diagram is modified from "Uses of

Environmental Isotopes" by T. B. Coplen in REGIONAL GROUND WATER QUALITY edited by W. M. Alley, pp. 227-254. Copyright © 1993. This material is used by permission of John Wiley & Sons, Inc.

Evaporation of water from surface-water bodies is a nonequilibrium process and the $\delta D/\delta^{18}O$ slope is usually between 3 and 6. This process can be described using the Craig–Gordon evaporation model (Craig and Gordon, 1965). The model takes into account the effect of relative (temperature normalized) humidity on isotopic fractionation during evaporation. If the vapor space is saturated, the process is an equilibrium reaction. For relative humidities of less than 100%, the process is a kinetic reaction in which diffusive isotope fractionation is an important factor. The greater the degree of undersaturation, the greater is the kinetic effect.

Water–rock interactions also affect isotopic compositions. Interactions between geothermal waters and rocks lead to changes in isotopic compositions. Because rocks have very little hydrogen, the exchange only affects the oxygen isotopes. Rocks have $\delta^{18}O$ values in the range of +2‰ to + 14‰. Geothermal waters interacting with country rocks will thus become enriched in $\delta^{18}O$, the degree of enrichment depending in part on the temperature at which the interaction is taking place. Recall that fractionation factors approach 1 as temperature increases. At sufficiently high temperatures, and assuming that isotopic equilibrium has been achieved, the $\delta^{18}O$ value of the water should approach that of the country rock. At low temperatures a common diagenetic reaction, the hydrolysis of silicate minerals, also leads to changes in isotopic compositions. These diagenetic reactions usually lead to a decrease in the $\delta^{18}O$ value of the water and an increase in the δD.

The sum total of these various isotopic interactions is to produce waters with different isotopic signatures. Thus, it may be possible to determine the contributions of various sources to ground or surface waters using stable isotopes (Case Study 6–4).

CASE STUDY 6–4 Sources of Groundwater in the Albuquerque, New Mexico, Area

A major area of concern in arid and semiarid regions is the source and recharge rate of groundwaters because groundwater is often a major water source. Lambert and Balsley (1997) determined the hydrogen and oxygen isotopic composition of water from municipal wells in Albuquerque, New Mexico. The results of this study were compared to δD values determined in an

earlier study. The δD and $\delta^{18}O$ values plot in two clusters along the meteoric water line (MWL) (Figure 6–C4–1) and define two end members for the groundwater system. The less negative cluster was named the eastern domain and was inferred to be derived from runoff from the Sandia and Manzano mountains along the eastern edge of the basin. The other cluster was named the central basin domain, which may partly consist of seepage from the Rio Grande river. Samples from two of the wells (Figure 6–C4–1) do not fall on the MWL and have excess deuterium of 5‰. The authors concluded that these waters were emplaced during climatic conditions different from the present day and may represent a separate groundwater reservoir. The authors also found that δD values along the eastern and western margins of the basin had become more negative over a ten-year period, suggesting an expansion of the central basin domain waters. Pumping at multiple depths in two wells showed that there were significant variations in isotopic compositions between different levels, indicating that the vertically stacked groundwaters have very little interconnection. It was suggested that long-term pumping tests could be used to determine the degree of interconnectivity between the various groundwater intervals; i.e., because the various levels have different isotopic compositions, changes in isotopic composition during pumping would indicate the movement of water between the different intervals.

Source: Lambert and Balsley (1997).

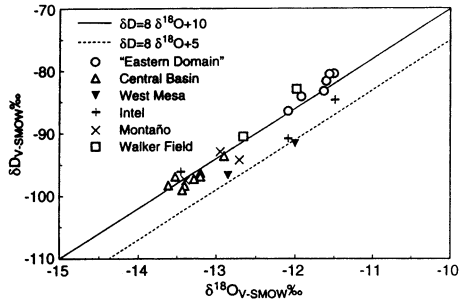

Figure 6–C4-1 *δD and $\delta^{18}O$ values for groundwaters from the Albuquerque Basin showing the various groundwater domains. From Lambert and Balsley (1997).*

EXAMPLE 6–7 *A dam and reservoir were constructed on a river in Arizona. River water sampled from a point 40 km downstream from the dam has $\delta D = -44.6‰$ and $\delta^{18}O = -3.6‰$. The river water has two sources, groundwater recharge and overflow from the dam. The isotopic composition of the groundwater is $\delta D = -38‰$ and $\delta^{18}O = -4.5‰$ (A in Figure 6–6). Because of evaporative water loss from the reservoir behind the dam, the isotopic composition of the water*

discharged from the reservoir is δD = −49‰ and $\delta^{18}O$ = −3.0‰ (B in Figure 6–6). Because these are the only two sources of water for the river, the resulting river water will be a simple mixture of the two end members. Calculate the groundwater component of the river flow.

Because we are using two isotopes, we can write two mass balance equations:

$$\text{For deuterium: } X\ \delta\text{D}_{\text{groundwater}} + Y\ \delta\text{D}_{\text{reservoir}} = \delta\text{D}_{\text{river}}$$

and

$$\textit{For oxygen: } X\,\delta^{18}O_{groundwater} + Y\,\delta^{18}O_{reservoir} = \delta^{18}O_{river}$$

where X is the contribution from the groundwater system and Y is the contribution from the reservoir. Substituting the appropriate values gives two simultaneous equations that can be solved for X and Y.

$$\text{For deuterium: } X(-38) + Y(-49) = -44.6$$
$$\text{For oxygen: } X(-4.5) + Y(-3.0) = -3.6$$

Solving gives X = 0.40 and Y = 0.60; 40% of the current stream flow represents groundwater input.

Climate Change Because the fractionation of hydrogen and oxygen isotopes is temperature sensitive, it has been possible to reconstruct past climatic conditions from stable isotope measurements on ice cores. Ice cores have been obtained from Greenland and Antarctica, and the results of these studies are reported in a number of papers (e.g., Dansgaard et al., 1969, 1971; Johnson et al., 1972). In brief, the isotopic composition of snow at high latitudes reflects the prevailing air temperature (Figure 6–7). Declining air temperatures lead to more negative δD and $\delta^{18}O$ values, and increasing air temperature leads to less negative δD and $\delta^{18}O$ values. During Southern Hemisphere summers (dates in Figure 6–7), ambient temperature increases are marked by less negative $\delta^{18}O$ and δD values. During Southern Hemisphere winters, $\delta^{18}O$ and δD values become more negative. The snow ultimately forms glacial ice, and if the ice stratigraphy is not disrupted, it is possible to map past temperature changes (Figure 6–8). A confounding variable is the isotopic composition of the ocean water from which the original water vapor is derived. During an ice age a significant amount of water is removed from the ocean and stored on the continents. This leads to an increase in the δD and $\delta^{18}O$ values for ocean waters (they become less negative),

and thus the water vapor becomes less negative. In this case, at constant air temperature, we would expect to see an increase in the δD and $\delta^{18}O$ values for snow, which would be interpreted as atmospheric warming. In practice, temperature changes generally outweigh this effect so that the direction, if not the absolute magnitude, of the temperature change is correct. Another point of contention is the meaning of the relative temperature changes; e.g., do they simply reflect local conditions, such as a change in the prevailing wind direction, or do they reflect global changes? If a reliable geochronology is available for ice cores collected in the Northern and Southern hemispheres, the presence of the same temperature variation in cores from both hemispheres is interpreted to represent a global variation, whereas the presence of a temperature variation in cores from only one hemisphere is interpreted to represent more local changes. In Figure 6–8, the Byrd Station (South Pole) and Camp Century (Greenland) ice cores are seen to show similar variations in $\delta^{18}O$ for the last 80,000 years, suggesting that the temperature changes are global. The increase in $\delta^{18}O$ during the last 10,000 years represents the global warming following the end of the last ice age. The lower $\delta^{18}O$ values found between 10,000 and 70,000 B.P. reflect the colder global temperatures during the last ice age. Climate change will be considered further in Chapter 8.

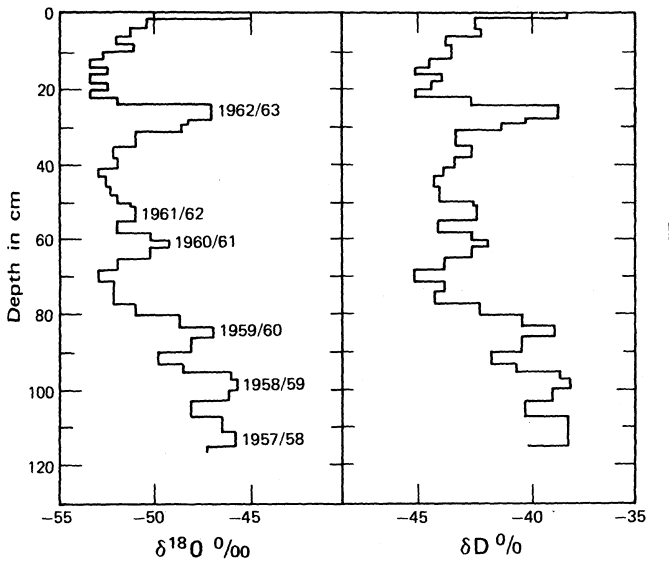

Figure 6–7 Seasonal variations in $\delta^{18}O$ and δD in snow and firn at the South Pole. From PRINCIPLES OF ISOTOPE GEOLOGY, 2nd Edition by G. Faure. Copyright © 1986. This material is used by permission of John Wiley & Sons, Inc.

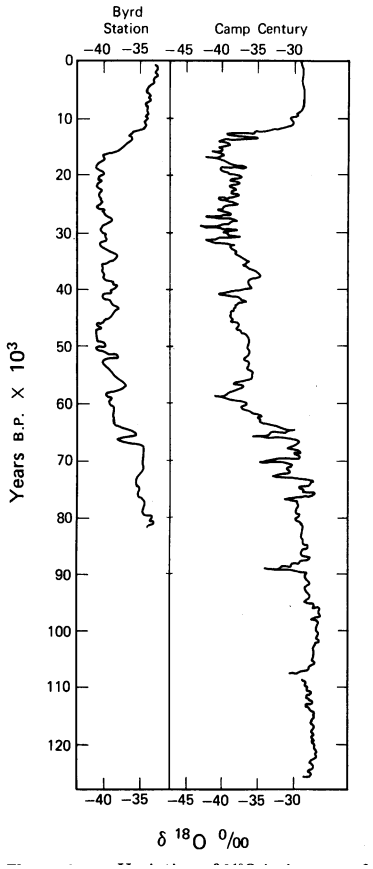

Figure 6–8 Variation in $\delta^{18}O$ in ice cores from Byrd Station and Camp Century. From PRINCIPLES OF ISOTOPE GEOLOGY, 2nd Edition by G. Faure. Copyright © 1986. This material is used by permission of John Wiley & Sons, Inc.

Carbon

Carbon occurs in a number of reservoirs (Figure 6–9), each with a characteristic range of $\delta^{13}C$ values. With respect to the PDB standard, most of the carbon at or near the earth's surface is enriched in ^{12}C relative to the standard; i.e., $\delta^{13}C$ values are negative. For the modern atmosphere, $\delta^{13}C = -7‰$**.** Both coal (petroleum is similar to coal) and methane are isotopically more negative than the present-day atmosphere. Thus, the addition of CO_2 to the atmosphere by the burning of fossil fuels leads to more negative values for $\delta^{13}C$. The $\delta^{13}C$ values for plants depend on the biochemical pathway used for carbon fixation (Deines, 1980). Most plants use the Calvin cycle (C_3) and have $\delta^{13}C$ in the range –24 to –37‰. Tropical grasses, marine aquatics, and desert and salt marsh plants use the Hatch-Slack cycle (C_4) and have $\delta^{13}C$ in the range −9 to −24‰. Some algae,

cacti, and succulents use the CAM (Crassulacean acid metabolism) cycle and have $\delta^{13}C$ values in the range −12 to −30‰. In principle, it is possible to use differences in $\delta^{13}C$ to distinguish between organic matter produced by the C_3 or C_4 cycles. Carbon occurs in the aquatic environment as DIC (dissolved inorganic carbon) and DOC (dissolved organic carbon).

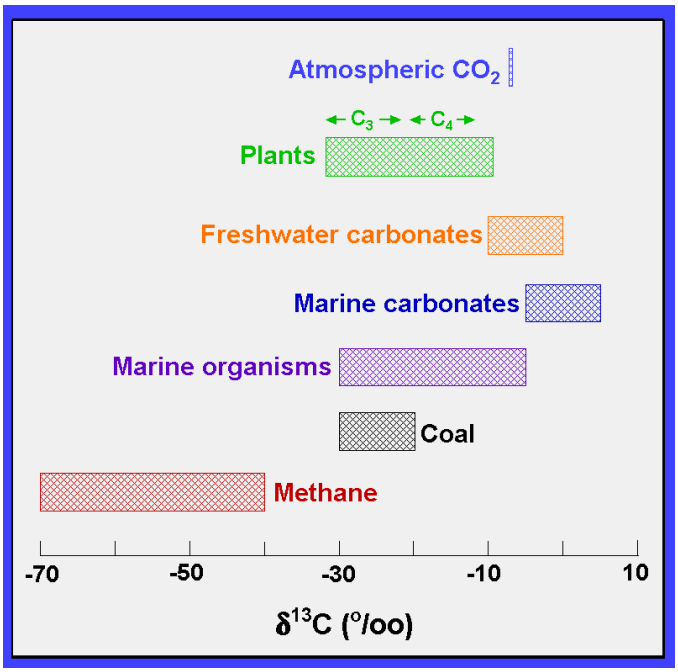

Figure 6–9 Range of $\delta^{13}C$ values for different carbon reservoirs.

DIC in Aqueous Systems The isotopic behavior of carbon in aqueous systems is complex. The major sources of carbon in water are carbonate minerals, organic matter, and atmospheric CO_2. The relative importance of these sources is a function of the system; e.g., atmospheric CO_2 is generally a minor source for groundwater systems but an important source for rivers, lakes, and the ocean. The isotopic composition of the total dissolved carbon in solution, and the isotopic composition of $CaCO_3$ in equilibrium with the solution, is a function of the temperature and pH (which affects the relative abundance of carbonate and bicarbonate ions) of the solution.

A number of authors (Deines et al., 1974; Grootes et al., 1969; Mook et al., 1974; Turner, 1982) have investigated the isotopic fractionation of carbon between CO_2 gas and CO_2 dissolved in solution, bicarbonate and carbonate ions, and solid calcium carbonate. Each species has its own fractionation factor, and hence the isotopic composition of the solution is a function of the relative

proportions of the different species. The empirical equations, based on experimental results, of Deines et al. (1974) are given in Table 6–8 and graphically illustrated in Figure 6–10.

Table 6–8 Fractionation Factors for Carbonate Species Relative to Gaseous CO_2*

H_2CO_3	$1000 \ln \alpha = -0.91 + 0.0063 \times 10^6/T^2$
HCO_3^-	$1000 \ln \alpha = -4.54 + 1.099 \times 10^6/T^2$
CO_3^{2-}	$1000 \ln \alpha = -3.4 + 0.87 \times 10^6/T^2$
$CaCO_3$ (s)	$1000 \ln \alpha = -3.63 + 1.194 \times 10^6/T^2$

*From Deines et al. (1974).

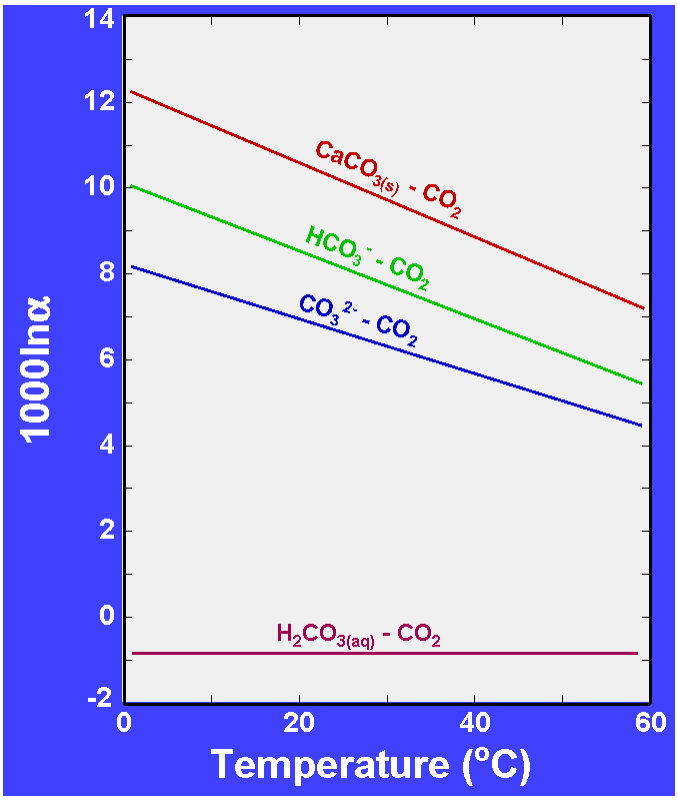

Figure 6–10 Isotopic fractionation factors, relative to CO_2 gas, for carbonate species as a function of temperature. Deines et al. (1974).

For $CO_{2\ (aq)}$ in equilibrium with $CO_{2\ (g)}$, the offset in the delta value can be calculated from the

following equation (Mook et al., 1974):

$$\varepsilon = -0.373 \times 10^3 / T + 0.19‰ \quad (6\text{–}52)$$

The calculated value (ε) is the difference between the $\delta^{13}C$ value for $CO_{2\ (g)}$ and $CO_{2\ (aq)}$. This offset is always negative, so the CO_2 in solution is always isotopically heavier than the coexisting CO_2 gas. In all of these equations, temperatures are in K.

EXAMPLE 6–8 *Calcium carbonate is precipitating at 25°C in equilibrium with atmospheric CO_2 ($\delta^{13}C$ = −7.0‰). Calculate the $\delta^{13}C$ for the carbonate. From Table 6–8,*

$$1000 \ln \alpha = -3.63 + 1.194 \times 10^6 / T^2 = -3.63 + 1.194 \times 10^6/(298.15)^2 = 9.8$$
$$\ln \alpha = 9.8 \times 10^{-3}$$
$$\alpha = 1.00985$$

Using equation 6–46 and rearranging,

$$\delta^{13}C_{\text{(carbonate)}} = 1.00985(-7.0 + 1000) - 1000 = 2.8‰$$

The carbonate is enriched by 2.8‰ in ^{13}C.

As was discussed in Chapter 3, the distribution of carbonate species in solution is a function of the pH of the solution (Figure 3–2). Because isotopic fractionation factors are different for each carbonate species, the relative abundance of the species will determine the $\delta^{13}C$ for the solution. For example, at pH = 4, $H_2CO_{3\ (aq)}$ is the dominant species in solution and the $\delta^{13}C$ of the DIC will be determined by the fractionation of carbon between $H_2CO_{3\ (aq)}$ and $CO_{2\ (g)}$. At pH = 8, the dominant species in solution is HCO_3^-, and the $\delta^{13}C$ of the DIC will be determined by the fractionation of carbon between HCO_3^- and $CO_{2\ (g)}$.

Another important factor controlling the isotopic composition of DIC is whether the system is open or closed to CO_2. In a closed system, there is no mass transfer across boundaries, whereas in an open system, there is mass transfer across boundaries. A confined aquifer would be an example of a closed system and the ocean is an example of an open system (there is free exchange of CO_2 between the atmosphere and the ocean).

EXAMPLE 6–9 *The ocean is an open system. For the present-day atmosphere, $\delta^{13}C$ = −7.0‰. Average ocean water has a pH ≈ 8.2. With reference to Figure 3–2, at this pH bicarbonate ion is*

the dominant species; thus, the $\delta^{13}C$ for oceanic DIC will be the same as the bicarbonate $\delta^{13}C$. Given a surface temperature of 10°C, calculate the $\delta^{13}C$ value for the bicarbonate ion.

Using the equation for the bicarbonate ion in Table 6–8, at 10°C α = 1.00921 and using equation 6–46 and rearranging,

$$\begin{aligned}\delta^{13}C_{\text{(bicarbonate)}} &= 1.00921(-7.0+1000)-1000 \\ &= 2.1‰ \text{ (for oceanic DIC)} \quad \blacksquare\end{aligned}$$

EXAMPLE 6–10 *A confined limestone aquifer (closed system) has a pH of 8. For the limestone, $\delta^{13}C$ = 0‰; for the CO_2, $\delta^{13}C$ = −25‰ (the soil CO_2 is from C_3 vegetation). At this pH the dissolution reaction for limestone can be written*

$$CaCO_3 + CO_2 + H_2O \rightarrow Ca^{2+} + 2HCO_3^-$$

In a closed system, $\delta^{13}C$ is a function of the relative amounts of CO_2 and $CaCO_3$ and their $\delta^{13}C$ values. In this case, the relative proportions of CO_2 and $CaCO_3$ are 1:1, which yields a final DIC value of −12.5‰. Because bicarbonate ion is the dominant species in solution, it will also have $\delta^{13}C$ = −12.5‰. ■

Sources of Methane Methane sources include petroleum, methane produced from kerogen at elevated temperatures (thermogenic), methane produced by bacterial action (either fermentation of acetate or reduction of CO_2), methane produced by the pyrolytic decomposition of organic material using heat energy derived from a magmatic source (geothermal), and abiogenic methane derived from the mantle. In terms of carbon and hydrogen isotopes, each of these potential sources has a different isotopic signature (Figure 6–11). Hence, it would, for example, be possible to distinguish between methane derived from petroleum and methane derived by bacterial reduction. With reference to Figure 6–11, it is seen that methane from petroleum would be isotopically heavier, in terms of carbon, than methane from bacterial reduction. If the methane in groundwater was derived from both sources, then the observed isotopic composition would fall on a mixing line between the two end members. As another example, consider the source(s) of methane in deep ocean waters. The isotopically heaviest methane is derived from the mantle. This type of methane has been observed in hydrothermal systems associated with the midocean ridges. In deep ocean waters, which are isolated from the atmosphere and are therefore not in equilibrium with atmospheric methane, it would be possible to determine the amount of mantle-derived methane

contributing to the total methane content of the deep waters. Case Study 6–5 (p. 192) illustrates how carbon isotopes can be used to distinguish leachate water from a landfill from natural (uncontaminated) water.

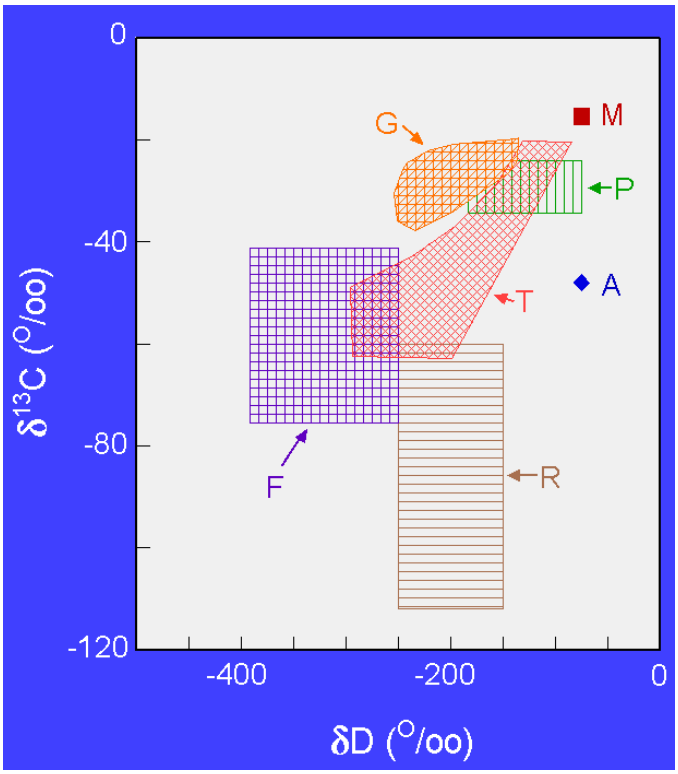

Figure 6–11 ^{13}C and deuterium isotopic values for methane from various sources and reservoirs. M—abiogenic (from the mantle), P— petroleum, A—atmosphere, G—geothermal (pyrolitic from interaction with magmatic heat), T—thermogenic (from kerogen at elevated temperatures), F—acetate fermentation (bacterial), and R—CO_2 reduction (bacterial). After Schoell (1984, 1988).

DOC in Aqueous Systems Dissolved organic carbon has multiple sources (see Chapter 5), including natural sources such as plant and animal remains and humic substances and manufactured organic compounds. To the extent that these compounds have unique isotopic signatures, they can be traced in the environment.

Tracers in Food Chains Because C_3 and C_4 plants have different isotopic characteristics, it is possible to trace the food sources for different organisms in a food chain. When plant material is consumed by a herbivore or an omnivore, the carbon is incorporated into the consumer with

minimal isotopic fractionation (e.g., about + 1‰). For example, maize is a C^4 plant ($\delta^{13}C \approx -15‰$) and wheat is a C_3 plant ($\delta^{13}C \approx -30‰$). This difference has been used by archaeologists to determine if the staple grain of an ancient population was maize or wheat. In combination with age-dating, $\delta^{13}C$ isotopic data have enabled archaeologists to determine when corn was introduced into the Americas.

CASE STUDY 6–5 Use of Isotopes to Characterize Landfill Leachates and Gases

Hackley et al. (1996) describe how isotopic systems can be used to characterize gases and leachates from landfills. The student should refer to this paper for a more complete discussion. During methanogenesis (the production of methane gas, CH_4), the hydrogen and carbon isotopes are fractionated. The two main processes are thermal decomposition and microbial decomposition of organic matter. Microbial decomposition can either proceed by acetate-fermentation or CO_2–reduction. These processes are described in Chapter 5. Each pathway produces isotopically distinct products (Figure 6–C5–1). Landfill methane gas has isotopic compositions typical of methane produced by acetate-fermentation. During methanogenesis there is a significant enrichment of deuterium in the leachate waters. This enrichment can be used to distinguish leachate water from natural waters (Figure 6–C5–2). The degree to which these isotopic distinctions are developed is a function of the time during which the processes have been active and the isolation of the landfill. During the early stages of biodegradation, the oxidation phases would be isotopically light ($\delta^{13}C = -10$ to $-35‰$), reflecting the isotopic composition of the original organic matter. As anaerobic decomposition proceeds, the values become more negative. Hence, gas and leachate from a relatively young landfill, or a young portion of a landfill, will not be distinctively different from natural sources. If the landfill is open to water, the shift in deuterium values due to methanogenesis will be overwhelmed by the input of natural waters. In Figure 6–C5–2 these two cases are illustrated by the points labeled C2 (where isotopically light groundwater was infiltrating and mixing with the leachate) and point C4 (a leachate sample from a new portion of the landfill).

The radiogenic isotopes of hydrogen and carbon may also be useful in identifying landfill gases and leachates. Both of these isotopes were produced during atmospheric testing of nuclear weapons and reached a maximum in 1962–1963 ^{14}C is enriched in landfill methane and leachates because most of the organic materials in landfills are young and have been influenced by the

increased ^{14}C content of the atmosphere due to weapons testing. Tritium values are often much higher than those to be expected from the input of local contemporaneous precipitation. These higher tritium values (ranging up to 8000 or more TU) may be due to the disposal of luminescent paints, which contain tritiated hydrocarbons, in landfills. Application of these isotopes to three different landfills in Illinois is illustrated in Figure 6–C5–3. Background-I was from surface water and groundwater near the surface and reflects the present-day input of these radiogenic isotopes. Backgrounds II and III were from confined aquifers approximately 30 meters below the surface. These aquifers presumably contain old waters that were not affected by the weapons-produced ^{3}H and ^{l4}C. The low background radioactivity for these two aquifers would increase the sensitivity of the isotope tracers.

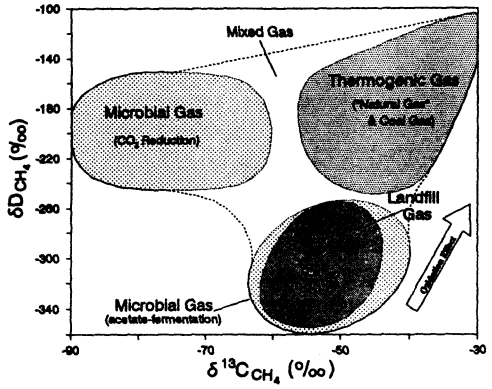

Figure 6–C5-1 *δD versus $\delta^{13}C$ for methane from different sources. Landfill methane plots in the field of acetate–fermentation.**

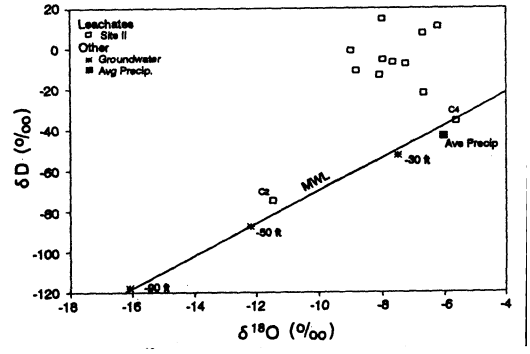

Figure 6–C5–2 *δD versus $\delta^{18}O$ for leachates from a municipal landfill in Illinois. The leachates are relatively enriched in deuterium compared to meteoric water. The two leachate samples (C2 and C4) that fall on the meteoric water line (MWL) represent leachate significantly diluted by*

*precipitation (C2) or from a recent portion of the landfill (C4).**

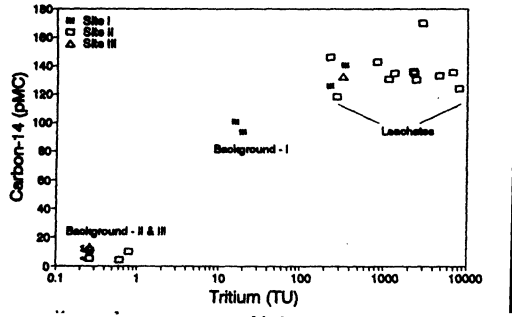

Figure 6–C5–3 *^{14}C and ^{3}H activities for leachates from three Illinois landfills. Background-I was determined from surface and shallow groundwater. Backgrounds-II and III were determined for confined aquifers at a depth of 30 m. Background-I shows the influence of present-day bomb-derived radiogenic isotopes.**

**Source: From "Environmental Isotope Characteristics of Landfill Leachates and Gases" by K. C. Hackley, C. L. Lui and D. D. Coleman, GROUND WATER; Vol. 34. No. 5, pp. 831–834 (Figures 5, 8, 9). September/October 1996. Reprinted from GROUND WATER with permission of the National Ground Water Association. Copyright 1996.*

Nitrogen

The main uses of nitrogen isotopes in the environmental field have been to trace the sources of nitrate pollution in ground and surface waters and to trace the sources of NH_3 and HNO_3 in rainfall (cars and factories versus agricultural). The processes controlling the isotopic composition of nitrogen are generally biological, rather than inorganic. Nitrogen isotopic values ($\delta^{15}N$) are reported relative to atmospheric air (AIR).

Nitrates in Surface and Ground Waters High abundances of nitrates in natural waters can cause adverse health effects and, if nitrogen is a limiting nutrient, can lead to eutrophication of rivers and lakes. Hence, there is an interest in the source of nitrates. The main sources of nitrates in surface and ground waters are fertilizer, animal or human waste, natural soil organic matter, nitrogen fixation, and rain. Nitrogen isotopes, in combination with other isotopes, have been used to elucidate which of these source(s) is contributing nitrates to the aqueous environment. These studies have been particularly useful in the identification of fertilizer or human and animal waste

sources. Because the nitrogen in fertilizer is extracted from the atmosphere, it has $\delta^{15}N = 0‰ \pm 2‰$. Animal and human waste has $\delta^{15}N = 15‰ \pm 10‰$. Thus, in principle, it is possible to distinguish between fertilizer- and waste-derived nitrates (Case Study 6–6). During denitrification, the $\delta^{15}N$ value of the residual nitrate increases, and it eventually becomes indistinguishable from the $\delta^{15}N$ value of manure. For this reason, better separation of sources is achieved if the oxygen in the nitrate is also analyzed. The oxygen in fertilizer will have $\delta^{18}O = +23‰$ (the $\delta^{18}O$ value for atmospheric oxygen), and for manure $\delta^{18}O = -10‰ \pm 10‰$ (oxygen derived from water). Denitrification is represented by the following equation:

$$4NO_3^- + 5CH_2O \rightarrow 2N_{2\,(g)} + 5HCO_3^- + H^+ + 2H_2O$$

Both nitrogen and oxygen isotopes are fractionated during denitrification, although the effect is greater for nitrogen. Because nitrogen is going into the gas phase, we would expect the residual nitrate to be enriched in the heavier isotope and the $\delta^{15}N$ value of the residual nitrate to increase. Oxygen shows a similar pattern, with an increase in the $\delta^{18}O$ value. These processes are graphically illustrated in Figure 6–12. If both sources are undergoing denitrification, it is possible to determine the relative contribution of each source to the water because the process is one of simple mixing. This is illustrated in Figure 6–12, in which both fertilizer and manure are contributing nitrates to a groundwater system. At some point, the fertilizer has an isotopic composition represented by point A and the manure has an isotopic composition represented by point B. A mixture of these two components would lie along the line A–B. In this case, the groundwater has a nitrate isotopic composition represented by point C. The relative percentage of each end member in the groundwater can be calculated from the lever law—e.g., the amount of A equals the distance C–B divided by the distance A–C. In this case, A provides 60% of the total nitrate to the groundwater.

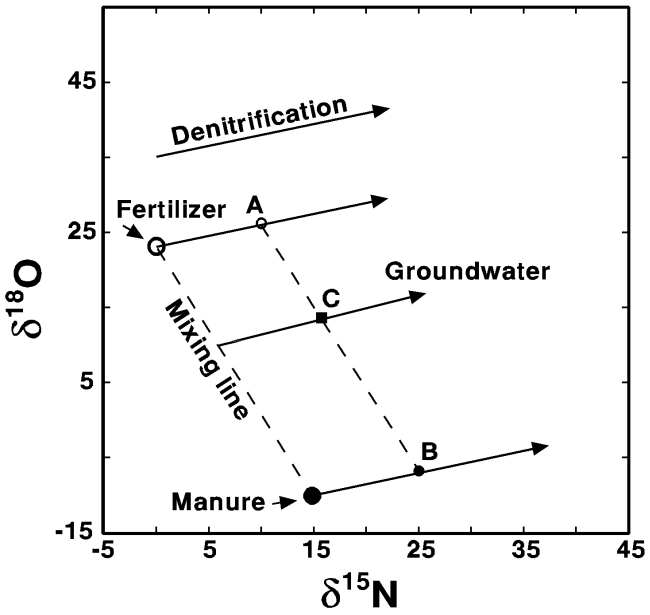

Figure 6–12 Determination of the relative importance of nitrate sources to a groundwater system. Two sources for nitrates are fertilizer and manure. Both are undergoing denitrification. A and B represent each source at a particular stage in the denitrification process. C is the isotopic composition of the nitrate in the groundwater due to simple mixing. In this example, approximately 60% of the nitrate is contributed by the fertilizer.

NH_4^+ and NO_3^- in Rain Anthropogenic sources—fossil fuel combustion and biomass burning—account for 65% of the total NO_x input to the atmosphere, and 56% of this 65% is due to fossil fuel combustion in automobile engines and power plants (Berner and Berner, 1996). NO_x has a residence time of about 6 days in the atmosphere and is then removed as HNO_3, a locally important component of acid rain. NH_4^+ (ammonium ion) is produced by the interaction of ammonia gas (NH_3) with water. The major continental sources of atmospheric ammonia are (1) bacterial decomposition of animal and human waste (45%), (2) bacterial decomposition of nitrogenous organic matter in soils (20%), (3) fertilizer (8%), (4) burning of coal (<<1%), and (5) biomass burning (3%). The remaining 24% is contributed by sea surface release (Berner and Berner, 1996). NO_x derived from fossil fuel combustion has $\delta^{15}N$ values in the range −10 to +5‰, and ammonia derived from the bacterial decomposition of animal and human wastes has $\delta^{15}N$ values in the range −15 to +30‰. In favorable circumstances, it may be possible to distinguish

between combustion and waste-decomposition sources of rainwater N.

CASE STUDY 6–6 Nitrogen Isotopes as Indicators of Nitrate Sources in Minnesota Sand-Plain Aquifers

Sand-plain aquifers, consisting of Quaternary-age glacial out-wash sands with interlayered clay, silt, silty sand, and gravel, underlie approximately 32,000 km^2 of central Minnesota and are important sources of water for irrigation and drinking. The aquifers are generally less than 30 m thick and are mainly recharged by the infiltration of precipitation. Thus, they are vulnerable to contaminants derived from the surface. In about 20% of the wells, nitrate concentrations exceed the recommended limit of 10 mg L^{-1} (as N). Komor and Anderson (1993) used nitrogen isotopes to identify the source of nitrates in groundwaters underlying five types of land-use areas: feedlot, cultivated-irrigated, cultivated-nonirrigated, residential with septic system, and natural. In general, various nitrate sources can be characterized as follows: nitrates from animal wastes, $\delta^{15}N$ = +10 to +22‰; nitrate from natural organic material in soil, $\delta^{15}N$ = +4 to +9‰; and nitrate from commercial fertilizers, $\delta^{15}N$ = −4 to +4‰;. These values can be changed during transport through the zone of aeration and the aquifer. Many of these processes lead to an increase in the $\delta^{15}N$ value of the residual nitrate. A total of 51 wells from the five land-use areas were sampled. The results of the nitrogen isotopic analyses are shown in Figure 6–C6–1. $\delta^{15}N$ values of greater than +22‰ found in some feedlot wells were attributed to denitrification. The samples from the residential area that showed high $\delta^{15}N$ values were believed to reflect leakage from septic systems. In general, cultivated areas in which both manure and fertilizer were applied had higher $\delta^{15}N$ values. For the cultivated-nonirrigated areas, the $\delta^{15}N$ values did not reflect the type of fertilizer (inorganic versus manure) applied to the fields. The authors suggested that this difference was due to the lower amount of water received by the nonirrigated fields. The nitrogen fertilizer added to the field would spend a longer period of time in contact with the natural soil material and would tend to homogenize with the soil nitrates. For the irrigated fields, the greater amount of water delivered during the growing season would wash much of the nitrate out of the soil horizon, thus diminishing the residence time of nitrates in the soil. On a qualitative basis, it should be possible to identify the source(s) of nitrates occurring in groundwater from the sand-plain aquifers.

Source: Komor and Anderson (1993).

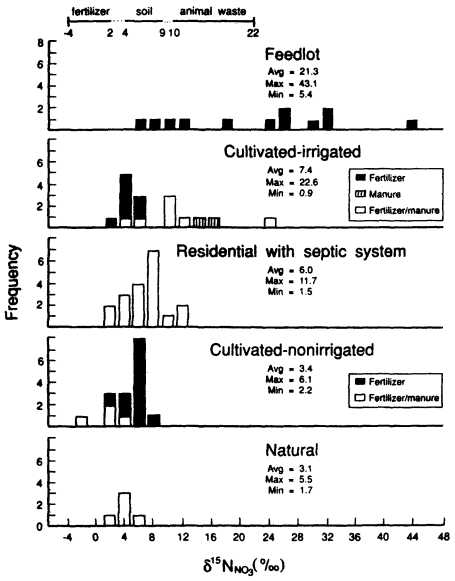

Figure 6–C6–1 *$\delta^{15}N$ values for groundwaters from various land-use areas. Forms of nitrogen applied to cultivated areas are shown on the diagram. From "Nitrogen Isotopes as Indicators of Nitrate Sources in Minnesota Sand-Plain Aquifers" by S. C. Komor and H. W. Anderson, GROUND WATER; Vol. 31, No. 2, p. 266 (Figure 3). March/April, 1993. Reprinted from GROUND WATER with permission of the National Ground Water Association. Copyright 1993.*

Sulfur

Sulfur isotope compositions are reported in terms of the $^{34}S/^{32}S$ ratio in parts-per-thousand relative to the CDT (Canyon Diabolo troilite) standard. Two major processes are responsible for variations in $\delta^{34}S$: reduction of sulfate to hydrogen sulfide by anaerobic bacteria, which results in the enrichment of hydrogen sulfide in ^{32}S, and various exchange reactions, which result in ^{34}S being concentrated in the compound with the highest sulfur oxidation state. The major sources of sulfate are ocean water, the dissolution of evaporites, oxidation of sulfide minerals, and atmospheric precipitation of sulfate. The major sources of sulfide are ore deposits, volcanic emanations, reducing environments, and the reduction of sulfate. Each of these sources has a characteristic range of $\delta^{34}S$. Sulfur is the major contributor to acid rain, so the source of the sulfur in the atmosphere has been an area of ongoing interest. Figure 6–13 shows the range of $\delta^{34}S$ values for sources of atmospheric sulfur. Under certain circumstances, the difference in the $\delta^{34}S$ values for the different sources can be used to determine the relative importance of each source to the total

atmospheric burden of sulfur. This is often done by determining the $\delta^{34}S$ values of local sulfur sources and then comparing these to the measured atmospheric $\delta^{34}S$ values. An example of such an approach is given in Case Study 6–7.

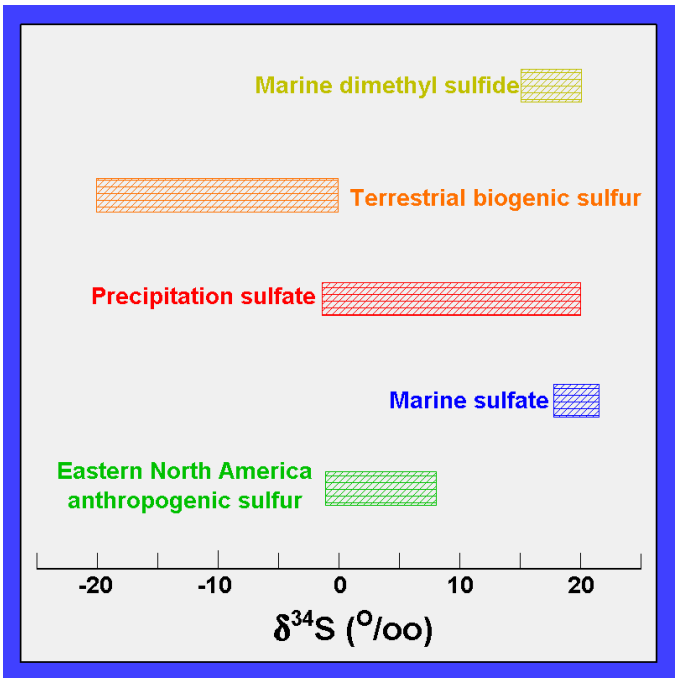

Figure 6–13 Range of $\delta^{34}S$ values for sulfur sources that contribute to atmospheric sulfur.

CASE STUDY 6–7 Sources of Sulfur Gases in Salt Lake City Atmosphere

Jensen (1972) identified three major sources for the sulfur gases found in Salt Lake City air:

Sulfur from oil refineries + automobiles: $\delta^{34}S$ = + 16‰ (S1)

Sulfur from copper smelters: $\delta^{34}S$ = + 1‰ (S2)

Bacteriogenic sulfur (H_2S) from Great Salt Lake: $\delta^{34}S$ = + 5.3‰ (S3)

When the smelters were operating, $\delta^{34}S$ = + 1.5‰ near the smelters and $\delta^{34}S$ = + 3.1‰ in Salt Lake City proper. This suggests that the major source of atmospheric sulfur was the smelters ($\delta^{34}S$ is near 1‰), but the significance of the other two sources for Salt Lake City was unknown. During a strike by smelter workers, $\delta^{34}S$ = + 5.3‰ near the smelters and +6.4‰ in Salt Lake City. Because the measured $\delta^{34}S$ value near the smelters is identical to the bacteriogenic sulfur value, the data indicate that the smelters and bacteriogenic sulfur are the only sources of sulfur for the

atmosphere in the vicinity of the smelters. When the smelters are operating,

$$\begin{aligned} x\ \mathrm{S2} + (1-x)\cdot \mathrm{S3} &= +1.5‰ \\ (x)(1) + (1-x)(5.3) &= 1.5 \end{aligned}$$

where x is the percent of sulfur contributed by the smelters. Solving for x, we get 0.88 (i.e., 88% of the sulfur is from the smelters). The remaining 12% represents the bacteriogenic input. For Salt Lake City, while the smelter workers were on strike, the only sulfur sources were the oil refineries + automobiles and bacteriogenic sulfur. Setting x = the oil refinery + automobile component,

$$\begin{aligned} x\ \mathrm{S1} + (1-x)\cdot \mathrm{S3} &= +6.4‰ \\ (x)(16) + (1-x)(5.3) &= 6.4 \end{aligned}$$

Solving for x, we get 0.10 (e.g., 10% of the sulfur is from the refineries + automobiles). The remaining 90% represents the bacteriogenic input. When the smelters are operating, all three sources contribute to the sulfur gases in the Salt Lake City atmosphere. From the observations made when the smelters weren't operating, we know that the relative contributions of S1 and S3 gave $\delta^{34}S = 6.4‰$. Setting ST = %S1 + %S3 = 6.4, we can write the following equation for the sulfur content of the Salt Lake City air when the smelters are operating:

$$\begin{aligned} x\ \mathrm{ST} + (1-x)\cdot \mathrm{S2} &= +3.1‰ \\ (x)(6.4) + (1-x)(1) &= 3.1 \end{aligned}$$

Solving for x gives 0.39 (e.g., 39% of the total sulfur in the Salt Lake City atmosphere comes from the combination of refineries + automobiles and bacteriogenic sulfur). The remaining 61% comes from the smelters. Refineries + automobiles contribute 10% of ST, so the percent contribution of refineries and automobiles to the Salt Lake City atmospheric sulfur is 4%. The other 35% (of ST) comes from bacteriogenic sulfur. Thus, for Salt Lake City 4% of the atmospheric sulfur comes from the oil refineries and automobiles, 35% from bacteriogenic sulfur, and 61% from the copper smelters. From this analysis it is clear that any significant reduction in the total sulfur burden of the Salt Lake City atmosphere can only be achieved by controlling the smelter emissions. This has, in fact, happened through the closure of some of the smelters and the installation of emission control devices on the remaining smelters.

Source: Jensen (1972).

For the United States, the major sources of anthropogenic sulfur are electricity generation (67%)

and industry (smelting and refining) (14%) (Berner and Berner, 1996). There are regional variations in the relative contributions of these sources. For example, in the western United States, metal smelters, particularly those in Arizona and New Mexico, contribute about 70% of the total anthropogenic sulfur.

The sulfur isotopic characteristics of the principal fossil fuels, petroleum and coal, vary on a deposit-by-deposit basis. In the case of petroleum, Thode and Monster (1965) concluded that petroleum is enriched in ^{32}S by about 15‰ relative to contemporaneous marine evaporites. They attributed this enrichment to the action of sulfur-reducing bacteria at the time of deposition of the sediment and during the subsequent formation of the petroleum. The source of the sulfur is marine sulfate. The isotopic composition of marine sulfate has varied during the Phanerozoic from + 10 to + 30‰ (Holser and Kaplan, 1966). Hence, petroleum formed at different times will have different $\delta^{34}S$ values, and given the 15‰ enrichment in ^{32}S, these values would be in the range of -5 to 15‰. In the case of coal, sulfur is present as sulfide minerals, sulfate, elemental sulfur, and organically bound. Each of these forms has different isotopic characteristics, and the $\delta^{34}S$ values of coal are highly variable and depend on the relative amounts of each component. For these reasons, it is difficult to draw any general conclusions as to the sulfur isotopic compositions of the fossil fuels. Therefore, $\delta^{34}S$ values need to be determined for each possible anthropogenic source.

Mixing

Binary Isotopic Mixing If we mix materials from two different isotopic reservoirs to form a material of intermediate composition, there are several possible relationships. For example, if we mix leachate from a dump with uncontaminated groundwater to produce a contaminated groundwater, in terms of hydrogen and oxygen isotopes, this mixing process can be described by the following equation:

$$\delta_M = \delta_A f_A + \delta_B(1 - f_A) \qquad (6\text{–}53)$$

where δ_A and δ_B are the isotopic values for the end members, δ_M is the isotopic value for the mixture, and f_A is the fraction of end member A in the mixture. This simple equation applies when the elemental concentrations are the same in the end members and the mixture. This would be the case for both hydrogen and oxygen in this example. However, note that if one of the end members was a brine, the concentrations of hydrogen and oxygen would not be the same in each end

member; i.e., on a weight/weight basis there would be less water in a kg of brine and hence less hydrogen and oxygen.

Continuing with the leachate example, if the element of interest is sulfur and the concentration of sulfur is different in the two end members, then concentration must be taken into account when doing the mixing calculations. In this case, we would use the following equation:

$$\delta_{\mathrm{M}} = \delta_{\mathrm{A}} f_{\mathrm{A}} (A/M) + \delta_{\mathrm{B}} (1 - f_{\mathrm{A}})(B/M) \qquad (6\text{–}54)$$

where A, B, and M are the concentrations of the element (or ion) in end member A or B or the mixture M; δ_{A}, δ_{B}, and δ_{M} are the corresponding isotopic values; and f_{A} is the fraction of end member A in the mixture. If we solve equation 6–54 for various mixtures of A and B, a plot of the sulfur isotopic ratio versus sulfur abundance will yield a hyperbola, characteristic of simple binary mixing. In the case of simple binary mixing, a plot of the isotopic ratio versus the reciprocal of the species concentration will yield a straight line (see problem 6–53).

Multi-End-Member Mixing of Chemical Species If the mixture involves more than two end members, the problem becomes a bit more complicated. However, if the end members can be identified, the composition of the resulting mixture can be calculated for any combination of end members. For example, if there were three end members—A, B, and C—that were mixed in the proportion 20A:30B:50C, one would first solve for a mixture of A and B (M′) and then for a mixture of M′ and C. The mixture of A and B (M′) would consist of 40% A and 60% B. The final mixture (M) would consist of 50% M′ and 50% C. On a graphical plot any mixture formed from these three end members would fall within a compositional triangle defined by the three end members (Example 6–11, Figure 6–14). The relative proportions of the end members can be determined by the application of the ***lever rule***, a useful tool for determining relative proportions when data are presented graphically. Example 6–11 illustrates how the lever rule is applied to a multi-end-member mixing problem.

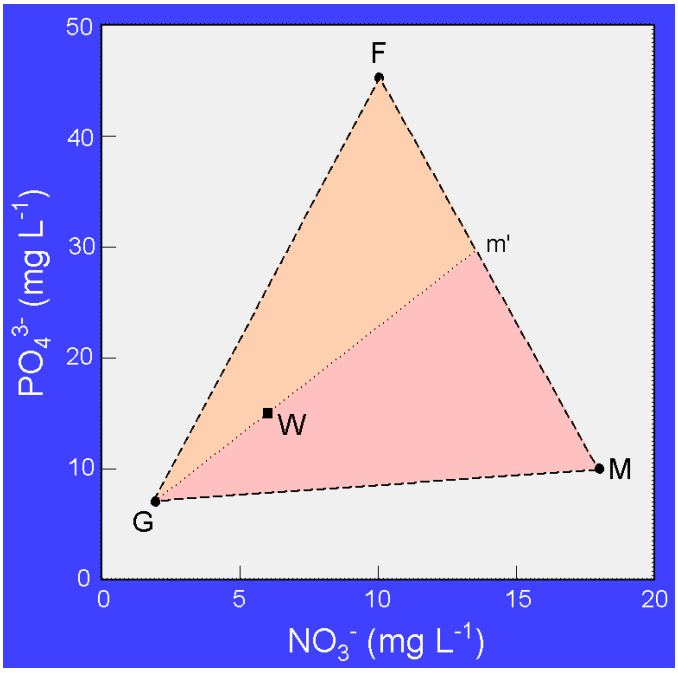

Figure 6–14 Plot of PO_4^{3-} versus NO_3^- in water samples from feedlot runoff (M), cultivated fields (F), uncontaminated groundwater (G), and contaminated well water (W). The sample of contaminated well water falls within the triangle defined by compositions M, G, and F, indicating that this sample is a mixture of these three compositions. The relative proportions of each end member can be determined by applying the lever rule (see Example 6–11).

EXAMPLE 6–11 *Elevated concentrations of phosphate and nitrate are found in a water well. There are two potential sources of phosphate and nitrate in the region, runoff from a feedlot and runoff from fertilized cultivated fields. Water samples collected in the immediate area of each of these sources give the following results: feedlot runoff (M),* $PO_4^{3-} = 10\ mg\ L^{-1}$ *and* $NO_3^- = 18\ mg\ L^{-1}$*; and runoff from cultivated fields (F)* $PO_4^{3-} = 45\ mg\ L^{-1}$ *and* $NO_3^- = 10\ mg\ L^{-1}$ *. For uncontaminated groundwater (G),* $PO_4^{3-} = 7\ mg\ L^{-1}$ *and* $NO_3^- = 2\ mg\ L^{-1}$*. For the well water (W),* $PO_4^{3-} = 15\ mg\ L^{-1}$ *and* $NO_3^- = 6\ mg\ L^{-1}$*. These four compositions are plotted in Figure 6–14. Note that the contaminated well water falls within the composition triangle defined by the three end members. We can determine the proportion of each end member in the sample by applying the lever rule. The proportion of uncontaminated groundwater in the sample is determined by measuring the distance Wm′ and dividing this distance by Gm′. The ratio is 0.64 and*

the proportion of groundwater in the sample is 64%. Note that the relative proportion of a particular component in a mixture is the distance from the mixture to the opposite component divided by the total distance between the two components. This follows from the observation that W is closer to component G than component m′. Thus, component G must be the major contributor to the mixture. The remaining 36% consists of runoff from the feedlot and the cultivated fields. This proportion can be determined as follows: measure the distance Fm′ and divide by the total distance FM. The resulting ratio is 0.44. Thus, of the remaining 36%, 44% is feedlot runoff, and feedlot runoff constitutes 16% (36% × 0.44) of the well water sample. The remaining 20% is runoff from the cultivated fields. To check your result, calculate the well water composition using the graphically determined proportions: $PO_4^{3-} = (0.64)(7) + (0.16)(10) + (0.20)(45) = 15 \text{ mg L}^{-1}$, *and* $NO_3^- = (0.64)(2) + (0.16)(18) + (0.20)(10) = 6 \text{ mg L}^{-1}$. ■

Paleothermometry

In a previous section we considered the reconstruction of past climates (e.g., temperatures) using ice cores. These measurements have been successfully extended back several hundred thousand years (see Chapter 8). The oldest obtainable information is ultimately limited by the depth at which the ice begins to flow, and the internal stratigraphy of the ice record is therefore lost. In order to look further back into the climatic record, we need other types of paleothermometers.

Urey (1947) suggested that the distribution of oxygen isotopes between water and calcium carbonate could be used to determine the temperature of ancient oceans, and such measurements were subsequently done by Urey et al. (1951). Although not without problems, as will be described, this has become a widely used paleothermometer. The basic equilibria have already been described in equations 6–41 to 6–43. The isotopic relationship between the temperature of the water and the coexisting calcite was experimentally determined by Epstein et al. (1953), and the subsequently modified version of the equation (Craig, 1965) is given here:

$$t\ (^{\circ}\text{C}) = 16.9 - 4.14(\delta_c - \delta_w) + 0.13(\delta_c - \delta_w)^2 \qquad (6\text{–}55)$$

where δ_c is the $\delta^{18}O$ value for calcite (relative to PDB) and δ_w is the $\delta^{18}O$ value for water (relative to SMOW). Problems with the paleothermometer include isotopic disequilibrium between the shell material and the water, postdeposition changes, and variations in the isotopic composition of the water. These problems have been addressed by using only species that seem to achieve isotopic

equilibrium for isotopic measurements and by independently determining the isotopic composition of the water. Freshwater shows such a wide range in isotopic ratios that freshwater organisms are not suitable for paleotemperature determinations. Ocean isotopic ratios are less variable, but recall from our earlier discussion that removal (glaciation) or addition (melting of glaciers) of water to the oceans will change the $\delta^{18}O$ values of seawater. Because the temperature of the deep ocean remains relatively constant (i.e., there is no variation in isotopic fractionation due to temperature changes), isotopic measurements done on benthic organisms can be used (assuming a particular temperature) to determine the $\delta^{18}O$ value of the coexisting water. Given the sum total of the corrections and assumptions that must be made in order to use this paleothermometer, most investigators use the results of such measurements to indicate relative, rather than absolute, changes in ocean temperatures. Cast Study 6–8 illustrates the application of pale-othermometry to an environmental question.

CASE STUDY 6–8 Stable Isotope and Heavy Metal Variations in the Shells of Mussels as an Indicator of Pollution in Lake Erie

Al-Asasm et al. (1998) analyzed the shells of Dreissena polymorpha, an exotic freshwater bivalve species found in the Great Lakes, for stable isotopes (carbon and oxygen) and heavy metals (Pb, Cd, Mn, Fe, Mg, V, and Cu). The organisms were collected from the western end of Lake Erie, near the mouth of the Detroit River. The organisms have a 3- to 9-year lifespan and show rapid growth. The shells have distinct growth layers due to seasonal variations—rapid growth in the summer, slow growth in the winter. Mollusks tend to concentrate heavy metals in their shells. Thus, they are potentially sensitive indicators of changes in heavy metal concentrations in the aquatic environment.

Calculations were done to determine if the aragonite shells of Dreissena polymorpha were formed in isotopic equilibrium with Lake Erie waters. For oxygen, the equation of Anderson and Arthur (1983) was used:

$$t\ (^{o}\mathrm{C}) = 19.0 - 3.52(\delta^{18}\mathrm{O}_{a} - \delta^{18}\mathrm{O}_{w}) + 0.13(\delta^{18}\mathrm{O}_{a} - \delta^{18}\mathrm{O}_{w})^{2}$$

where t is the temperature, $\delta^{18}O_a$ (PDB) is the isotopic composition of the shell, and $\delta^{18}O_w$ (SMOW) is the isotopic composition of the water. For Lake Erie, average water temperature is 25.8°C and $\delta^{18}O_w$ is –7.03‰ (SMOW). For the aragonite shells, the authors calculated an

equilibrium of $\delta^{18}O_w$ = –7.36‰ (PDB), in good agreement with the measured values. Substitution of the authors' values into the equation yields a temperature of 20.2°C, suggesting that there may be an error in the paper with respect to the water temperature used in the calculation. A similar calculation was done for carbon using the equation of Rubinson and Clayton (1969):

$$\delta^{13}C_{(\text{aragonite})} = \delta^{13}C_{(HCO_3)} + 1.85 + 0.035(t - 25^{o}C)$$

where t is temperature and the isotopic ratios are reported relative to PDB. The authors' estimated $\delta^{13}C$ equilibrium value is −0.92‰. This value is 1 to 1.5‰ heavier than the values measured for the shells. Thus, the shells are depleted in ^{12}C with respect to the equilibrium value. The authors considered a number of possible reasons for this difference. One of the more significant factors might be the influx of isotopically lighter organic carbon from domestic and industrial sewage.

It was found that the heavy metal concentrations in the shells tended to follow changes in the isotopic ratios. When the shells were enriched in the heavier isotope, there was an increase in the total metal concentration. The isotopic changes were correlated with changes in temperature, the enriched values reflecting higher temperatures, higher metabolic activity for the organisms, and increased mobility of the metals. Shells collected near the mouth of the Detroit River had higher total heavy metal concentrations, a response to their proximity to an anthropogenic source.

Source: Al-Asasm et al. (1998).

QUESTIONS AND PROBLEMS

1. The $^{84}_{38}Sr$ nucleus contains how many protons? how many neutrons?

2. Distinguish between *radioactive*, *radiogenic*, and *stable* isotopes.

3. Define *half-life.*

4. What is *RBE*?

5. What is meant by the term *event dating*?

6. Define *tritium unit* (TU).

7. Discuss the corrections that must be made in the tritium-helium-3 dating method. You may want to refer to the paper of Schlosser et al. (1989) in order to give a complete answer for this

question.

8. With reference to Case Study 6–1, why did the authors use multilevel sampling wells?

9. Groundwaters isolated from the atmosphere prior to 1952 can't be dated by the tritium method. Why not?

10. Why is the tritium content of air over the oceans lower than that of air over the continents?

11. How and why will the burning of fossil fuel affect the ^{14}C content of the atmosphere?

12. What factors affect the atmospheric concentration of ^{14}C? Explain how we can correct ^{14}C ages in order to account for these variations.

13. Why would contamination of a sample by modern carbon be a major problem when dating *old* samples using the ^{14}C method? How would the modern carbon affect the measured age (i.e., would it be younger or older)?

14. In terms of radioactive isotopes, what is *secular equilibrium*?

15. Explain the basic concept of a *disequilibrium dating method.* Give an example.

16. What do we mean when we say the activity of a particular radioactive isotope is *supported*?

17. In Case Study 6–2, the authors concluded that the Pb maximum found in the sediments of Lake Constance was not due to the burning of leaded gasoline. Why did the authors reach this conclusion, and what sources did they suggest for the Pb and why?

18. Explain the reasons for the variation in strontium isotopic ratios in different rock samples. How can these variations be used to identify the source(s) of groundwaters?

19. Why would Pb in galena formed at different times in earth history have different isotopic ratios?

20. In terms of the fractionation of stable isotopes, distinguish between *equilibrium* and *kinetic* reactions.

21. Explain why, during the evaporation of water, the vapor is enriched in ^{16}O relative to the liquid.

22. What is the *isotopic fractionation factor*?

23. Why and how does the isotopic fractionation factor vary as a function of temperature?

24. Why do we use isotopic standards?

25. Explain why snow falling at the North Pole is isotopically lighter, in terms of hydrogen and oxygen, than rain falling at the equator.

26. Distinguish between the *mean global meteoric water line* and *local meteoric water lines.*

27. With reference to Case Study 6–4, how could changes in isotopic compositions during the pumping of a well be used to determine the degree of interconnectivity of various groundwater intervals?

28. How can carbon and oxygen isotopes be used to determine temperature variations during the last 100,000 years of earth history? Answer this question in the context of data obtained from Greenland ice cores.

29. How does the addition of CO_2 to the atmosphere by the burning of fossil fuels affect the $\delta^{13}C$ values and why?

30. Why is the pH of a solution an important factor in determining the $\delta^{13}C$ of DIC?

31. An archaeologist uncovers prehistoric human remains in the U.S. southwest. Isotopic analysis of these remains yields $\delta^{13}C = -14‰$. Was the staple food crop for people living at this time wheat or maize? How did you determine your answer?

32. With reference to Case Study 6–5, how could leachate waters from a landfill be distinguished from natural waters?

33. What is the effect of denitrification on the $\delta^{15}N$ value of manure?

34. With reference to Case Study 6–6, how can nitrogen isotopes be used to distinguish between groundwaters contaminated by runoff from feedlots versus groundwaters contaminated by leakage from residential septic systems?

35. List and describe the major processes that affect the isotopic composition of sulfur. How do each of these processes affect the $\delta^{34}S$ value?

36. List and discuss the factors that affect the carbonate paleothermometer.

37. Exposure to radon gas leads to a dose of 1×10^{-4} rad being deposited in a basement dweller's lungs. Calculate the biological exposure. Be sure to take into account the nature of the

ionizing radiation. For small doses, a millirem (mrem = 1×10^{-3} rem) is often used. This may be a more appropriate unit for this calculation than the rem.

38. A groundwater sample is collected from a deep aquifer. No tritium activity is observed in the sample. The activity of ^{14}C in the atmosphere is 13.56 dpm g^{-1} of carbon. The observed ^{14}C activity in the water sample is 4.54 dpm g^{-1} of carbon.

a. What is the significance of the absence of tritium in the sample? Why is it important to check for the presence of tritium before using the ^{14}C method to date a water sample?

b. Calculate the age of the water sample.

c. Suppose the water sample had been in contact with Devonian limestone and that 60% of the total carbon was derived by dissolution of this limestone. What effect would this have on the calculated age of the water? Recalculate the age of the water sample accounting for the *limestone* carbon.

39. Schlosser et al. (1989) measured tritium and ^{3}He abundances in a well at Liedern/ Bocholt, West Germany. Their data are reproduced in the accompanying table. The data were all decay-corrected to a sampling date of May 6, 1987. Column 1 gives the depth below the groundwater table. When answering the questions, don't forget that all these measurements are corrected to 1987—i.e., all ages are relative to 1987.

Depth (m)	^{3}H (TU)	^{3}He (TU)	$^{3}H + {}^{3}He$ (TU)
0.5	23.1	2.7	25.8
1.5	26.7	5.9	32.6
2.5	37.8	20.2	58.0
4.5	55.3	42.2	97.5
5.5	53.0	76.6	129.6
10.5	29.7	66.1	95.8
12.5	30.5	51.7	82.2

Depth (m)	^{3}H (TU)	^{3}He (TU)	^{3}H + ^{3}He (TU)
16.5	20.5	41	61.5
27.5	3.0	13.6	16.6

a. The highest tritium values for rainfall occurred in 1963. At what depth is this tritium found in the groundwater? What is the age of the groundwater at this depth?

b. For each depth, calculate the tritium age. Does the calculated tritium age at the depth that corresponds to the tritium maximum agree with the age you inferred for this depth in part (a)? If it doesn't, what are some possible reasons for the discrepancy?

c. Plot depth versus the tritium age. What can you conclude from this plot?

40. Stute et al. (1997) determined the ages of groundwater samples at various distances from the Danube River. Recharge to the surficial aquifer is dominated by bank infiltration. Part of their data compilation, for deep wells presumably unaffected by mixing with locally recharged groundwater, is given in the accompanying table.

Distance Danube (km)	^{3}H (TU)	^{3}He (TU)	^{3}H + ^{3}He (TU)
2.0	23.1	7.9	31.0
3.5	24.1	5.5	29.6
8.6	46.5	84.2	130.7
11.2	68.5	164.5	233.0
12.0	79.5	277.1	356.6
14.2	63.6	204.4	268.0
14.8	74.8	298.5	373.3

Distance Danube (km)	^{3}H (TU)	^{3}He (TU)	$^{3}H + {}^{3}He$ (TU)
18.3	3.9	19.4	23.3
29.5	< 1	4.3	< 5.3

This problem is most easily done on a spreadsheet.

a. Calculate the age of each of the groundwater samples.

b. Plot the ages of the groundwater samples versus their distance from the Danube River.

c. Calculate the horizontal flow velocity for the groundwater away from the Danube River.

41. ^{14}C ages for carbonate and organic samples need to be corrected for isotopic fractionation. The following equation is used to calculate the correction:

$$A_{corr} = A_{meas}\left[1 - \frac{2(25 - \delta^{13}C_{PDB})}{1000}\right] \text{dpm g}^{-1}$$

where $\delta^{13}C_{PDB}$ is the delta value for the sample. A mollusk shell was collected from Pleistocene lake deposits in southern New England. For this specimen, $\delta^{13}C_{PDB} = -9.0‰$ and ^{14}C activity = 0.9 dpm g^{-1}. Use the present-day ^{14}C activity of the atmosphere as the activity at $t = 0$. Calculate the age of the shell.

42. Rember et al. (1993) measured the concentrations of ^{137}Cs in the bottom sediments of Medicine Lake, northern Idaho. Heavy-metal-laden tailings from the Coeur d'Alene mining district were deposited in this lake. Tailings were deposited during floods as well-stratified, heavy-metal, contaminated silts on the lake bottom. Atmospheric testing of nuclear bombs, the source of ^{137}Cs, began in 1951 and reached a maximum in 1964. ^{137}Cs is first detected in the varved sediments at a depth of 30–32 cm and the ^{137}Cs maximum occurs at a depth of 16–18 cm.

a. Calculate the average sedimentation rate for the varved sequence.

b. The last layer of varved sediment is encountered at a depth of 10-12 cm. What is the age of

this sediment layer?

c. Tailings ponds were installed in the mining district in 1968. Have these ponds reduced the input of tailings to Medicine Lake? Explain.

43. The following ^{230}Th activities were determined for a deep-sea sediment core:

Depth (cm)	^{230}Th (dpm g^{-1})
0	65.5
20	33.6
40	17.4
60	9.6
80	5.7
100	3.5
120	2.4

a. Calculate the sedimentation rate.

b. If the ^{231}Pa activity is 6.9 dpm g^{-1} at 10 cm, what would the activity be at 50 cm?

44. Das et al. (1994) used the activity of ^{210}Pb in lake sediments to determine the sedimentation rate for a number of lakes in northern India. The data for two of the lakes are reproduced here along with the average ^{226}Ra activity due to the presence of ^{238}U in the sediments.

Core no.	Depth (cm)	Total ^{210}Pb (dpmg^{-1})	^{210}Pb excess (dpm g^{-1})
Nainital	0-6	2.628	2.468
Lake NT-1	6–12	2.117	
	12-18	2.000	
Average ^{226}Ra = 0.16 dpm g^{-1}			

Core no.	Depth (cm)	Total ^{210}Pb ($dpmg^{-1}$)	^{210}Pb excess ($dpm\ g^{-1}$)
Sattal Lake	0–6	17.916	
ST-1	6–12	11.090	
	12–18	4.510	
	18–24	3.622	
	24–30	0.822	
Average ^{226}Ra = 0.822 dpm g^{-1}			

a. Complete the data table.

b. For each lake, plot the log of ^{210}Pb excess versus arithmetic depth. For the depth use the midpoint of each interval.

c. From the activity versus depth plots, calculate the average sedimentation rate for each lake. If you do this problem on a spreadsheet, you can use the curve-fitting function of the spreadsheet program to determine the slope of the activity versus depth curve.

d. The catchment area for one of these lakes has a relatively dense population; the other is sparsely populated. Which lake catchment has the low population density and why did you pick this lake?

45. With reference to Case Study 6–3, the average values for uncontaminated groundwater are AR = 1.5 and U = 15 μg L^{-1}, and for dilute raffinate AR = 1.05 and U = 100 μg L^{-1}. A groundwater sample collected peripheral to the site has AR = 1.2 and U = 35 μg L^{-1}. Calculate the percent raffinate in this groundwater sample.

46. For Greenland, average summer temperatures are 0°C and average winter temperatures are –30°C. The fractionation factors for $\delta^{18}O$ are: at –30°C, α = 1.0155; and at 0°C, α = 1.0112.

a. For Rayleigh fractionation, after 90% condensation (f = 0.1), calculate the $\delta^{18}O$ for the water vapor when condensation is occurring at 0°C and − 30°C. At the start of the condensation

process $(\delta^{18}O)_0 = -10‰$ for the water vapor.

b. Calculate the isotopic composition of snow formed during the summer and winter seasons.

47. Hubbard Brook, in the White Mountain National Forest, New Hampshire, has a pH of 4.9. Assuming that the waters of Hubbard Brook are in equilibrium with atmospheric CO_2 ($\delta^{13}C = -7.0‰$), for a water temperature of 20°C calculate $\delta^{13}C$ for the dissolved inorganic carbon (DIC).

48. The delta values for sulfur from different sources are (1) biogenic hydrogen sulfide = −2.0‰, (2) seawater sulfate = +20.0‰, and (3) sulfur in coal = +5.0‰. Case Study 6–7 may be of use in solving this problem.

a. An atmospheric aerosol collected over city X has $^{32}S/^{34}S = 21.78$. Calculate the delta value for this aerosol. What can you conclude about the source of the aerosol and the location of city X?

b. A coastal city has only two major sources of sulfur, rain derived from the ocean and sulfur derived from a coal-burning power plant. A sample of city air yields $\delta^{34}S = +14.0‰$. Calculate the percent sulfur in the city air that is derived from the power plant.

49. Grasby et al. (1997) investigated the hydrogen, oxygen, and sulfur isotope geochemistry of Nose Creek, a tributary to the Bow River in Alberta, Canada. Nose Creek flows southward through the town of Airdrie (25,000) and the city of Calgary (700,000) and enters the Bow River south of Calgary. The Bearspaw Reservoir, located on the Bow River, is the source of the municipal water supply for Calgary and Airdrie. Water samples were collected during the fall of 1993 and the spring of 1996. The results of the isotopic analyses are given here. For oxygen and hydrogen, SMOW was used as the standard; for sulfur, CDT was used as the standard.

Sample	Location	$\delta^{18}O_{(H_2O)}$	$\delta D_{(H_2O)}$	$\delta^{34}S_{(SO_4)}$	$\delta^{18}O_{(SO_4)}$
Nose Creek (Fall 1993)					
NC1-0893	North Airdrie	−12.51	−105.9	16.66	7.02
NC2-0893	Airdrie	−13.70	−120.3	7.88	3.97

Sample	Location	$\delta^{18}O_{(H_2O)}$	$\delta D_{(H_2O)}$	$\delta^{34}S_{(SO_4)}$	$\delta^{18}O_{(SO_4)}$
NC3-0893	North crossing	−14.00	−125.9	5.53	3.33
NC4-0893	South crossing	−15.18	−123.0	6.15	3.40
NC5-0893	Country Hills	−15.05	−122.2	4.61	0.63
NC6–0893	32nd Ave. NW	−17.50	−139.5	−5.89	−7.03
NC7-0893	Calgary Zoo	−18.19	−140.6	−6.25	−2.29
NC8-0893	Centre Street	−19.02	−141.4	−7.44	−3.66
Nose Creek (Spring 1996)					
NC1-0696	North Airdrie	−15.20	−121.9	—	3.90
NC2-0696	Airdrie	−15.40	−121.5	12.56	1.41
NC3-0696	North crossing	−15.40	−124.2	10.82	4.39
NC4-0696	South crossing	−15.50	−124.6	9.68	4.30
NC5-0696	Country Hills	−15.10	−120.3	7.21	1.08
NC6–0696	32nd Ave. NW	−15.20	−115.4	0.33	2.40
NC7-0696	Calgary Zoo	−15.30	−120.9	−1.02	0.37
NC8-0696	Centre Street	−17.80	−131.9	−0.83	0.68
Below Bearspaw Reservoir					
BR7-0893	Bowness	−18.80	−146.0	10.48	—

a. Plot the δD and $\delta^{18}O$ values listed in the table. Use different symbols to distinguish the spring and fall samples. Draw the local meteoric water line (LMWL) on the graph. The coordinates of the LMWL are δD = −100‰, $\delta^{18}O$ = −13.2‰ and δD = −160‰, $\delta^{18}O$ = −20.5‰. Also plot the Bowness sample on the graph using a distinguishing symbol.

b. From the graphical relationships, what can you conclude about the major source of the Nose

Creek waters during the spring and the fall? In making these interpretations keep in mind that evaporation will probably not be an important process for Nose Creek and that the Bow River (Bearspaw Reservoir) is the source of the municipal water supplies.

c. Plot $\delta^{34}S_{(SO4)}$ versus $\delta^{18}O_{(H2O)}$. Plot the spring and fall samples on the same graph using different symbols.

d. The two most likely sources of sulfur for Nose Creek are weathering of till and/or bedrock and an anthropogenic input. The Crossfield gas plant is located north of Airdrie. For the sour gas emitted from this plant, $\delta^{34}S = +25‰$. Between Airdrie and urban Calgary, A-horizon soils typically have $\delta^{34}S = +3$ to $+10‰$, and this is an agricultural area. Total S (pyrite + organic S) for the Balzac till, which underlies Calgary, has $\delta^{34}S = -25‰$. Based on the isotopic characteristics of the different sulfur sources, describe and explain the variations and patterns seen on the plot constructed in part (c).

50. For a stream draining a region underlain by granites, Sr = 0.06 mg L^{-1} and $^{87}Sr/^{86}Sr = 0.7200$. A tributary that drains a region underlain by carbonate rocks enters the stream. For the tributary, Sr = 0.4 mg L^{-1} and $^{87}Sr/^{86}Sr = 0.7092$. Immediately downstream from the tributary the following values are measured for the river water: Sr = 0.128 mg L^{-1} and $^{87}Sr/^{86}Sr = 0.7178$. Calculate the amount of tributary water added to the main river.

51. Fritz et al. (1994) measured the sulfur isotopic composition of leachate seeping from a closed landfill. For the leachate, $\delta^{34}S = +17‰$. Gypsum mined in the United States that is used for plaster board would have $\delta^{34}S = +20$ to $+30‰$, leading the authors to conclude that the breakdown of plaster board in the landfill was the source of the sulfate in the leachate. Deep and shallow groundwaters in the area have an average of $\delta^{34}S = +0.5‰$. Water from a shallow well downgradient from the landfill had $\delta^{34}S = +10.6‰$. If the concentrations of the SO_4^{2-} ions in the various solutions are as follows: leachate = 14 mg L^{-1}, uncontaminated groundwater = 2.4 mg L^{-1} and contaminated groundwater = 9.5 mg L^{-1}, calculate the percent leachate in the groundwater.

52. With reference to Case Study 5–5, Smirnov et al. (1998) identified three distinct groups of Lake Erie bottom sediments in terms of PAH content and $\delta^{13}C$. Two end members were identified, fluvial input from Detroit, Cleveland, and Buffalo and uncontaminated bottom

sediments (North Zone). A sample of Lake Erie bottom sediment has TPAH = 2351 ng g^{-1} and $\delta^{13}C = -26.4‰$. Calculate the percent fluvial component in this sample of bottom sediment.

53. In the upper reaches of a river, the drainage basin is underlain by granites. In the lower reaches of the river, the drainage basin is underlain by carbonate rock. The carbonate rock is first encountered at a distance of 30 km from the headwaters of the river. Measurements made at various downstream locations are given in the accompanying table.

a. Plot the $^{87}Sr/^{86}Sr$ ratio versus Sr concentration. Describe the shape of the resulting curve.

b. Calculate 1/Sr. Plot the $^{87}Sr/^{86}Sr$ ratio versus 1/Sr. Describe the shape of the resulting curve. Do the data fit a simple binary mixing model? Explain.

c. For waters in equilibrium with the granites, $^{87}Sr/^{86}Sr = 0.7200$ and Sr = 0.06 mg L^{-1}. For waters in equilibrium with the carbonate rocks, $^{87}Sr/^{86}Sr = 0.7092$ and Sr = 0.4 mg L^{-1}. Assuming simple binary mixing, calculate the proportion of carbonate-derived waters in the water sample collected at 70 km.

Distance (km)	Sr (mg L^{-1})	$^{87}Sr/^{86}Sr$
0	0.060	0.7200
10	0.060	0.7200
20	0.060	0.7200
30	0.060	0.7200
40	0.094	0.7154
50	0.128	0.7133
60	0.162	0.7120
70	0.196	0.7112
80	0.230	0.7106
90	0.264	0.7102

Distance (km)	Sr (mg L^{-1})	$^{87}Sr/^{86}Sr$
100	0.298	0.7099

54. Runoff from a feedlot and fertilized cultivated fields is entering a groundwater aquifer. Unpolluted groundwater samples have $PO_4^{3-} = 3\ mg\ L^{-1}$ and $NO_3^- = 1\ mg\ L^{-1}$. For the runoff from the feedlot, $PO_4^{3-} = 6\ mg\ L^{-1}$ and $NO_3^- = 18\ mg\ L^{-1}$, and for runoff from the cultivated fields, $PO_4^{3-} = 42\ mg\ L^{-1}$ and $NO_3^- = 11\ mg\ L^{-1}$. For the contaminated groundwater, $PO_4^{3-} = 9\ mg\ L^{-1}$ and $NO_3^- = 11\ mg\ L^{-1}$. Plot the data and determine the relative proportions of the three end members using the lever rule. Check your answer by using these proportions to calculate the composition of the contaminated groundwater.

55. The relationship between $\delta^{18}O$ and temperature for calcite in equilibrium with water has been determined experimentally. This relationship is represented by equation 6–55. This geothermometer has been used to track temperature changes in the world's oceans. One of the problems with the geothermometer is that changing climatic conditions can change the isotopic composition of seawater. One way to correct for this is to determine the isotopic composition of a benthic organism and use this value to estimate the seawater isotopic composition, assuming a constant temperature for the deep ocean. This seawater isotopic composition can then be used to determine surface seawater temperature using a pelagic organism.

a. A benthic organism has δ_c = +5.25‰. Assuming that the temperature of the deep ocean remains constant at 1°C, calculate the isotopic composition of the seawater in equilibrium with this shell. You will need to use the quadratic formula in order to solve this part of the problem.

b. A pelagic organism has δ_c = +2.5‰. Calculate the temperature of the surface water in equilibrium with this shell.

56. Price et al. (2000) determined the carbon and oxygen isotopic characteristics of belemnite genera from the early Cretaceous interval of the Speeton Clay Formation, Filey Bay, England. A subset of their data compilation is given here. The first column gives the height of

the sampled interval above the base of the section, arranged in normal stratigraphic order (youngest at the top). The approximate age of this section is 142 to 133 million years. The data for two belemnite species (*Hibolites* sp. and *Acroteuthis* sp.) are listed in the table. An analysis of their results led the authors to conclude that the isotopic data were consistent across these two species.

a. Calculate the paleotemperature for each belemnite sample using equation 6–55. Price et al. (2000) assumed that Early Cretaceous seawater had $\delta^{18}O = -1‰$.

b. Plot stratigraphic height (on the *y*-axis) versus $\delta^{13}C$ and $\delta^{18}O$. Draw smooth curves through the data points.

c. For each stage, plot the calculated temperature versus $\delta^{13}C$**.** If you've done these calculations on a spreadsheet, draw a linear regression line for each data subset.

d. From the plots constructed to answer parts (b) and (c), what conclusions can you draw about the relationship between paleotemperature and $\delta^{13}C$? Interpret the results. You may want to refer to the original paper.

Height from base (m)	Stage	Species	$\delta^{13}C$ (‰) (PDB)	$\delta^{18}O$ (‰) (PDB)	*T*(°C)
26.91	Late Hauterivian	*Hibolites* sp.	1.78	0.63	_____
25.53	Late Hauterivian	*Hibolites* sp.	1.76	0.50	_____
25.50	Late Hauterivian	*Hibolites* sp.	−0.13	0.10	_____
23.49	Early Hauterivian	*Hibolites* sp.	1.62	0.72	_____
22.00	Early Hauterivian	*Hibolites* sp.	1.18	0.46	_____
20.42	Early Hauterivian	*Hibolites* sp.	0.60	0.62	_____
19.14	Early Hauterivian	*Hibolites* sp.	1.60	−0.27	_____
19.02	Early Hauterivian	*Hibolites* sp.	1.23	0.59	_____
19.00	Early Hauterivian	*Hibolites* sp.	1.49	0.87	_____

Height from base (m)	Stage	Species	$\delta^{13}C$ (‰) (PDB)	$\delta^{18}O$ (‰) (PDB)	*T*(ºC)
18.71	Early Hauterivian	*Hibolites* sp.	1.30	−0.89	_____
18.57	Early Hauterivian	*Hibolites* sp.	1.89	0.21	_____
17.96	Early Hauterivian	*Hibolites* sp.	1.00	−0.46	_____
16.71	Early Hauterivian	*Hibolites* sp.	0.25	0.24	_____
16.26	Early Hauterivian	*Hibolites* sp.	0.81	0.40	_____
14.52	Early Hauterivian	*Hibolites* sp.	1.23	0.56	_____
12.33	Early Valanginian	*Acroteuthis* sp.	−0.27	−0.25	_____
11.81	Early Valanginian	*Acroteuthis* sp.	0.14	−0.60	_____
11.21	Early Valanginian	*Acroteuthis* sp.	−0.71	−0.29	_____
11.00	Early Valanginian	*Acroteuthis* sp.	1.30	−0.42	_____
10.56	Early Valanginian	*Acroteuthis* sp.	−1.38	−0.86	_____
9.84	Early Valanginian	*Acroteuthis* sp.	0.31	−0.08	_____
9.09	Early Valanginian	*Acroteuthis* sp.	0.79	0.47	_____
1.68	Late Ryazanian	*Acroteuthis* sp.	0.34	0.44	_____
1.63	Late Ryazanian	*Acroteuthis* sp.	−1.05	−0.06	_____
0.80	Late Ryazanian	*Acroteuthis* sp.	−0.22	0.37	_____

57. Jones and Young (1998) used laser ablation to measure the $\delta^{18}O$ isotopic composition of tooth enamel from the molar of a modern African elephant in Amboseli National Park, Kenya. Ten analyses were done through a 1750-μm section of tooth enamel parallel to the growth direction. The enamel growth rate was estimated to be 150 to 200 μm per month. Thus, the traverse represents approximately 1 year in the life of the elephant. For the local drinking

water (largely snowmelt from Kilimanjaro), $\delta^{18}O = -5‰$.

Ayliffe et al. (1994) give the following relationship for the fractionation of oxygen isotopes between water and tooth enamel: $\delta^{18}O_p = 0.94 \pm 0.1\delta^{18}O_w + 23.3 \pm 0.7$.

a. Calculate the $\delta^{18}O$ for the elephant's enamel.

b. Several segments of tooth enamel had $\delta^{18}O = 23‰$**.** These segments were formed during the wet season when meteoric water is the dominant source for drinking water. Calculate $\delta^{18}O$ for the meteoric water.

c. If only a bulk analysis had been done on this tooth, how would the estimated $\delta^{18}O$ for meteoric water in equatorial Africa differ from the actual $\delta^{18}O$?